Charles University
Faculty of Science

**Study program:** Physical Geography and Geology
**Studijní program:** Fyzická geografie a geoekologie


Benjamin James Stoker

# The dynamics of the north-western Laurentide Ice Sheet margin
# Dynamika severozápadního okraje Laurentinského ledovcového štítu

Doctoral dissertation

**Supervisor:** Mgr. Martin Margold, Ph.D.
**Co-supervisor:** Prof. Duane Froese
**Advisor:** doc. RNDr Zbyněk Engel, Ph.D.

Prague 2024

This page is left intentionally blank.

**Prohlášení:**

Prohlašuji, že jsem tuto disertační práci vypracovala samostatně a že jsem řádně citovala všechny použité informační zdroje a literaturu. Tato práce ani žádná její podstatná část nebyla předložena k získání stejného nebo jiného akademického titulu.

**Declaration:**

I declare that I compiled this doctoral dissertation independently and that I properly cited all the utilized information sources and literature. Neither the thesis nor any of its substantial parts has not been submitted to obtain the same or other academic degree.

05 February 2024, Prague.

_____

Podpis/signature

# Table of Contents

# Acknowledgements

First, I would like to extend my sincere gratitude to my PhD supervisors, Martin Margold and Duane Froese. My main supervisor, Martin, was patient and gave me the freedom to explore and develop the research topics that interested me. He was always available to provide support on everything from administrative procedures to fieldwork planning and shaping research projects. His approach allowed me to develop my research interests and ability to think independently and undertake a research project from start to finish. I am also grateful to my co-supervisor, Duane, for many insightful discussions throughout that helped shape my research. Duane always welcomed me into his research group to collaborate on fieldwork or simply be part of another research team and these valuable experiences taught me different ways to think and approach research problems. Their collective wisdom has been integral to the successful completion of this thesis and shaping my research abilities. I look forward to continuing to work together and collaborating on projects in the coming years.

I am deeply thankful to my colleagues whose collaboration and friendship have enriched my academic journey. In particular, over four years in Prague, Helen Dulfer helped me navigate the (often unnecessarily complicated) administrative systems of Charles University, and I am sure that I would have failed alone. Her collaboration on research was also essential. Not just the ability to always be able to discuss research issues but also the countless work hours we spent together mapping shorelines and lineations. Both Joe Young and Alejandro Alvarez always made me feel welcome at the University of Alberta and during multiple field campaigns. I learnt a lot about planning and undertaking field research in northern Canada from their help. I would also like to thank Sophie Norris who was always willing to share her knowledge and support me in developing research ideas. John Jansen also helped in the development of a, currently, unfinished project and has been a friend throughout this journey. During a research visit to Durham University, Chris Stokes provided more support and time than I could have ever expected, and I am grateful for everything I learnt while I was there. Finally, Rod Smith has always been incredibly open and honest in our discussions about the northwestern Laurentide Ice Sheet. His willingness to share research plans and discuss the Northwest Territories really deepened my understanding of the region and his review of my first manuscript taught me a lot.

Finally, I am deeply grateful to my family for their support throughout this journey. My parents have always given unconditional support that has allowed me to follow my passions and do something that I love. Without their encouragement and sacrifices, this would not have been possible. My sister, Laura, always helped me whenever I needed, including in helping learn how to use Word to format a CV. My partner, Aneta, has always been there over the last five years, despite a global pandemic, months spent half a world apart, and her own PhD worries. Her support and company have made the years in Prague incredible and made this accomplishment possible. I am incredibly grateful to them all.

The First Nations communities of northern Canada, where this research took place, are the traditional owners of the land and I am grateful for their support and cooperation during my research in the region. In particular, the Aurora Research Institute granted permission to undertake fieldwork and facilitated communication with First Nations communities.

I am immensely grateful to the funding agencies whose support made this research possible. Their financial assistance not only enabled me to pursue my academic aspirations but also provided the resources necessary to conduct meaningful research. I extend my sincere thanks to the NRCan Polar Continental Shelf Program and the Natural Sciences and Engineering Research Council of Canada, who supported fieldwork campaigns, Charles University Grant Agency project (GAUK project no. 122220), which provided both salary funding and fieldwork funding, the project Grant Schemes at Charles University (reg. no. CZ.02.2.69/0.0/0.0/19_073/0016935; START/SCI/055), which provided funding for salary costs, fieldwork, and research visits, and the Mount Everest Foundation, who supported a field campaign to the Mackenzie Mountains. Both the POINT Internationalization grant and POLENET provided funding to attend training courses during this PhD.

# Abstract:

The Laurentide Ice Sheet (LIS) was the largest ephemeral ice sheet in the Northern Hemisphere, reaching its all-time maximum during the last glacial cycle (~115 ka to ~11.7 ka) as it coalesced with the Cordilleran and Innuitian ice sheets over northern North America and the Canadian Arctic Archipelago. At its maximum extent it was comparable in size to the modern-day Antarctic Ice Sheet and may provide a useful analogue for understanding the long-term dynamics of ice sheets. There are considerable regional variations in our understanding of the deglaciation of the LIS. In particular, the northwestern LIS remains one of the most poorly understood sectors, as the latest reconstruction of this sector dates to the early 1990s and empirical constraints on the timing of deglaciation are sparse.

In this thesis, I reconstruct the deglaciation of the northwestern LIS from its local Last Glacial Maximum (LGM) position using numerical dating methods and glacial geomorphological mapping. I use a combination of high-resolution digital elevation models (DEMs) and satellite imagery to map the glacial geomorphology of much of the Northwest Territories, Canada, and reconstruct the ice margin retreat patterns, ice flow dynamics, and interaction of the northwestern LIS with other ice masses. This new information is published in four papers, of which I am leading three and co-authoring one. The glacial geomorphological map of the Mackenzie Mountains (paper I) maps the landforms produced by the LIS, the Cordilleran Ice Sheet, and the local montane ice masses into six categories: glacial lineations, lateral meltwater channels, undifferentiated meltwater channels, lateral meltwater spillways, eskers, and moraines. These landforms constrain the maximum extent and interactions between these ice masses in the Mackenzie Mountains. In paper II, the glacial geomorphological map focuses solely on the imprint of the northwestern LIS across the Northern Interior Plains and the Canadian Shield and records the changing ice flow and margin retreat patterns. There are twelve landform categories on this map: glacial lineations, subglacial ribs, crevasse fill ridges, major and minor moraine, hummocky terrain and ridges, marginal meltwater channels, major and minor meltwater channels, shear margin moraines, eskers ridges, glaciofluvial complexes, perched deltas, raised shorelines and aeolian dunes.

Using new terrestrial cosmogenic nuclide exposure ages from the central Mackenzie Valley, we reconstruct the timing of northwestern LIS deglaciation (paper III). Samples for cosmogenic nuclide dating were taken from erratics at six sites spanning a range of latitudes, longitudes and elevations to gain an insight into the pattern of ice margin retreat and to constrain the rate of ice sheet retreat and thinning. We combine these new constraints in a Bayesian framework with the pre-existing dates and find that deglaciation occurred ~1,000 years earlier than in previous reconstructions. Between ~14.9 and 13.6 ka, we identify a period of rapid ice sheet thinning associated with warming during the Bølling-Allerød. The large uncertainties in terrestrial cosmogenic nuclide exposure dating mean that we are unable to quantify a precise rate of ice sheet thinning. Our constraints necessitate a revision of the ice margin retreat pattern, with ice retreat from the central Mackenzie Valley (~63 - 65°N) occurring in an easterly direction, rather than the previously suggested southerly retreat pattern. Using numerical modelling simulations, we calculate a contribution of ~13.4 m to global mean sea level rise from the ice saddle region, with 11.2 m occurring between 16 ka and 13 ka. Finally, our constraints indicate that the Mackenzie Valley became ice-free after 13.6 ka (14.1 – 13.2 ka) with implications for the migration of flora and fauna between Beringia and North America and glacial lake drainage routes.

The dynamics of the ice drainage network during deglaciation have not previously been reconstructed. We use the flowset mapping approach to reconstruct the changes in ice flow dynamics using the glacial geomorphological map from paper II. Our reconstruction provides evidence of the changing ice source areas related to rapid thinning of the ice saddle during the Bølling–Allerød and the increasing dominance of the Keewatin Ice Dome. The ice stream network underwent rapid changes during deglaciation that are associated with climate-driven changes in the ice sheet surface slope and facilitated by the subglacial bed conditions and the presence/absence of a calving margin. The glacial landform record indicates that dynamic ice margin retreat dominated during deglaciation, with a clear zonation that reflects the changing thermal regime.


**Keywords:** Laurentide Ice Sheet, glacial geomorphology, flowset reconstruction, cosmogenic nuclide exposure dating, sea level rise, ice streams

# Abstrakt:

Laurentinský ledovcový štít byl největším z efemérních ledovcových štítů severní polokoule. Svého maximálního rozsahu dosáhl během posledního glaciálního cyklu (~115 ka až ~11,7 ka), kdy se spojil s Kordillerským a Inuitským ledovcovým štítem na severu Severní Ameriky a v Kanadském arktickém souostroví, a svou velikostí byl srovnatelný s dnešním Antarktickým ledovcovým štítem. Porozumění dynamice odlednění Laurentinského ledovcového štítu je cenné pro pochopení dlouhodobé dynamiky dnešních ledovcových štítů, ale v informacích o odlednění Laurentinského ledového štítu existují značné regionální rozdíly. Zejména severozápadní sektor Laurentinského ledovcového štítu zůstává jedním z nejhůře prostudovaných, protože poslední rekonstrukce tohoto sektoru pochází z počátku 90. let 20. století a množství empirických informací o chronologii odlednění v tomto sektoru je nedostatečné.

Tato práce rekonstruuje odlednění severozápadního sektoru Laurentinského ledovcového štítu z jeho posledního glaciálního maxima pomocí numerických datovacích metod a geomorfologického mapování. Glaciální geomorfologie velké části Severozápadních teritorií Kanady je mapována z digitálních modelů terénu s vysokým rozlišením a ze satelitních snímků a následně interpretována za účelem rekonstrukce dynamiky ústupu ledovcového štítu a interakce severozápadního sektoru Laurentinského ledovcového štítu s jinými ledovcovými masami. Tyto nové informace jsou publikovány ve čtyřech článcích, z nichž jsem hlavním autorem tří a spoluautorem jednoho. Článek „Glacial geomorphological map of the Mackenzie Mountains“ (článek I) mapuje tvary reliéfu vytvořené Laurentinským ledovcovým štítem, Kordillerským ledovcovým štítem a lokálním horským zaledněním. Tyto tvary reliéfu vymezují maximální rozsahy a interakci mezi těmito ledovcovými masami v Mackenzie Mountains během posledního zalednění. Druhý článek mapuje glaciální geomorfologii severozápadního sektoru Laurentinského ledovcového štítu v severní části Vnitřních rovin a na Kanadského štítu.

Článek č. 3 využívá kosmogenní Be-10 k datování ústupu Laurentinského ledovcového štítu z údolí řeky Mackenzie na jejím středním toku. Vzorky na datování byly odebrány z eratických balvanů na šesti lokalitách v rozpětí různých zeměpisných šířek a nadmořských výšek, aby data obsáhla jak ústup okraje ledovce, tak snižování jeho mocnosti během odlednění. Nová data jsou kombinována s existujícími chronologickými informacemi v bayesovském schématu a výsledky indikují, že k odlednění došlo přibližně o tisíc let dříve než uváděly dosavadní rekonstrukce. V období ~14,9 a 13,6 tisíc let před současností došlo k období rychlého poklesu povrchu ledovcového štítu v souvislosti s interglaciálem Bølling-Allerød. Poměrně velká nejistota spojená s datováním kosmogenním Be-10 ale způsobuje, že nejsme schopni určit přesnou míru poklesu povrchu ledovcového štítu v čase během tohoto období. Naše výsledky nicméně vyžadují revizi dosavadních rekonstrukcí ústupu okraje ledovcového štítu v rámci studijní oblasti, přičemž okraj ledovcového štítu ustupuje z centrálního údolí řeky Mackenzie (~63-65° s. š.) spíše východním směrem než dříve předpokládaným jižním směrem. Pomocí numerického modelování počítáme příspěvek ~13,4 m ke zvýšení globální hladiny moře z širší oblasti ledovcového sedla mezi Laurentinským a Kordillerským ledovcovým štítem, přičemž 11,2 m připadá na období mezi 16 a 13 tisíci lety před současností. Naše data následně indikují, že údolí řeky Mackenzie bylo odledněno 13,6 tisíc let před současností (14,1 - 13,2), což je údaj důležitý pro studie migrace flóry a fauny mezi Beringií a Severní Amerikou a pro studie směrů odtoku velkých, ledovcovým štítem hrazených jezer.

Dynamika ledovcového štítu během odlednění (tzn. primárně konfigurace ledovcových proudů, tzv. „ice streams“) nebyla dosud rekonstruována. Tato práce používá tzv. inverzních glaciálně geomorfologických metod k rekonstrukci dynamiky ledovcového štítu z mapovaných a interpretovaných glaciálních tvarů reliéfu (mapovaných v článku 2). Naše rekonstrukce nově dokládá migraci akumulační oblasti ledovcového štítu v důsledku zániku ledovcového sedla mezi Laurentinským a Kordillerským ledovcovým štítem. Změny v síti ledovcových proudů by dále ovlivněny měnícím se podélným profilem ledovcového štítu, který reagoval na klimatické výkyvy na konci pleistocénu. V důsledku měnícího se podélného profilu ledovcového štítu se měnil též teplotní režim na bázi ledovce, což mělo vliv na ledovcové proudy, a ty byly dále ovlivněny přítomností nebo absencí procesu telení do oceánu nebo hlubších ledovcových jezer. Podle naší intepretace mapovaných glaciálních tvarů reliéfu převažoval ve studijní oblasti během odlednění dynamický

ústup okraje ledovcového štítu (oproti stagnaci a odtávání „mrtvého ledu“). Jasná zonace mapovaných glaciálních tvarů reliéfu reflektuje měnící se teplotní režim na bázi ledovce.

**Klíčová slova:** Laurentinský ledovcový štít, glaciální geomorfologie, datování kosmogenními izotopy

# List of publications in the thesis:

| | |
|---|---|
| Paper I – | **Stoker, B.J.,** Margold, M. and Froese, D., 2023. The glacial geomorphology of the Mackenzie Mountains region, Canada. *Journal of Maps*, pp.1-12.<br><br>**Author contribution** – 90% - The geomorphological mapping and manuscript preparation were all undertaken by BJS under the supervision of MM and DF. |
| Paper II – | Dulfer, H.E., **Stoker, B.J.,** Margold, M. and Stokes, C.R., 2023. Glacial geomorphology of the northwest Laurentide Ice Sheet on the northern Interior Plains and western Canadian Shield, Canada. *Journal of Maps*, pp.1-18.<br><br>**Author contribution** – 30% - The geomorphological mapping for this publication was split evenly between HED and BJS. The manuscript was written principally by HED (50% contribution) with input from BJS. MM (10%) and CRS (10%) supervised the project. |
| Paper III – | Stoker, B.J., Margold, M., Gosse, J.C., Hidy, A.J., Monteath, A.J., Young, J.M., Gandy, N., Gregoire, L.J., Norris, S.L. and Froese, D., 2022. The collapse of the Cordilleran–Laurentide ice saddle and early opening of the Mackenzie Valley, Northwest Territories, Canada, constrained by 10 Be exposure dating. *The Cryosphere*, *16*(12), pp.4865-4886.<br><br>**Author contribution** – 40% - The project was conceptualised by MM and DF. The first field data collection was performed by MM, JY and DF, with BJS also involved in a second round of data collection. The data analysis and interpretation were performed by BJS. The Bayesian modelling was done by AJM with input from BJS and JY. The ice sheet modelling was done by LJG and NG. The cosmogenic nuclide exposure age lab processing was completed by JCG and AJH. The manuscript was written by BJS with input from all co-authors. |
| Paper IV – | Stoker, B.J., Dulfer, H.E., Stokes, C.R., Brown, V.H., Clark, C.D., Ó Cofaigh, C., Evans, D.J.A., Froese, D., Norris, S.L. and Margold, M. *in review.* The ice flow dynamics of the northwestern Laurentide Ice Sheet during the last deglaciation. Submitted to *The Cryosphere, Special Issue: Icy landscapes of the past.*<br><br>**Author contribution** – 40% - The flowset mapping procedure was performed by both BJS and HED. The reconstruction of ice flow evolution through time was undertaken by BJS with input from HED and MM throughout. The manuscript writing was principally undertaken by BJS, with part of the methods section written by HED. All co-authors contributed throughout the ice flow reconstruction and the data interpretation. |

I, Martin Margold, agree with the author contribution statements above _____

# 1.0 Introduction:

Anthropogenically-influenced changes in climate since the industrial era have had widespread impacts on the Earth system, including the near universal recession of glaciers and ice sheets (Rignot *et al.,* 2014; IPCC, 2019; Field *et al.,* 2014; Randle and Eckersley, 2015). This recession has led to a 0.2 (0.15 – 0.25) m rise (IPCC, 2019) in global mean sea level (GMSL) between 1901 and 2018 with the average rate of sea level rise increasing from 1.3 [0.6 to 2.1] mm $yr^{-1}$ between 1901 and 1971 to 3.7 [3.2 to 4.2] mm $yr^{-1}$ between 2018 and 2018 (IPCC, 2023). The Greenland and Antarctic ice sheets hold the potential to cause a further 65.66m of GMSL (IPCC, 2013). The future of these ice sheets also has consequences for the regional climate, for example, the input of freshwater from the melting Greenland Ice Sheet to the Atlantic Ocean may weaken the North Atlantic thermohaline circulation and cause cooling (Fichefet et al., 2003). An understanding of the drivers of deglaciation is key to accurately forecasting future rates of ice sheet retreat and the contribution to GMSL rise. Studies of modern observational glaciology have allowed us to understand the magnitude and drivers of current changes but are limited to the last century.

The gradual cooling trend throughout the Cenozoic period culminated in the development of continental-scale ice sheets in the Northern Hemisphere that grew and shrank to the pace of orbital cycles during the Quaternary period (the last ~2.58 Myr; Le Treut and Ghil, 1983; de Boer and Smith, 1994). These cyclical variations in ice volume are a key characteristic of the Quaternary and were the dominant contributor to past sea level changes, resulting in a sea level lowering of up to 130m during the Last Glacial Maximum (LGM; ~27 – 20 ka; Lambeck and Chappell, 2001). While climate oscillations drove ice sheet changes, ice sheet changes also caused feedback effects that influenced the ocean circulation patterns and global climate (Lambeck and Chappell, 2001; Rasmussen *et al.,* 2014). The reconstruction of these Quaternary ice sheets can provide empirical data to validate numerical ice sheet models and gain a deeper understanding of the long-term drivers of ice sheet retreat (Clark *et al.,* 2018; Ely *et al.,* 2021).

During the LGM, the Laurentide Ice Sheet (LIS) was located over eastern and central northern North America and coalesced with both the Cordilleran and Innuitian ice sheets farther west and north to form the North American Ice Sheet Complex (NAISC), which was the largest Northern Hemispheric ice mass with a GMSL equivalent volume of ~80 m (Dalton et al., 2023; Figure 1). During its maximum extent it blocked the migration of early humans and animals into North America (Froese et al., 2019), disrupted ocean circulation through cyclical events of high ice flux (Heinrich Events; Hemming, 2004; Broecker et al., 1993) and the ice sheet topography directly modulated the atmospheric circulation patterns (Löfverström et al*.,* 2014). Furthermore, climatic oscillations following the LGM provide an opportunity to understand the response of ice sheets to millennial-scale changes in climate.

The advance and retreat of the NAISC significantly modified the landscape through the erosion, transportation and deposition of material leading to an abundance of glacial landforms and sediments across much of northern North America (Fulton, 1989; Dyke, 2004). The landforms and sediments left behind following deglaciation provide an opportunity to reconstruct the past extent, advance and retreat patterns, and dynamics of former ice masses (Smith et al., 2006). Traditional studies employed field-based surveys to map the glacial geomorphology, but this process was revolutionised over the last decades by the availability of increasingly high-resolution datasets which provides a cost and time efficient method to map large areas of formerly glaciated terrain (Punkari, 1980; Clark, 1997; Kleman et al., 1997; Smith and Pain, 2011; Chandler et al., 2018). These maps can also be used to identify locations to target for geochronological methods to reconstruct the rates of ice sheet retreat (Chandler et al., 2018).

Within the LIS, the northwestern margin has received relatively little attention compared to the better studied southern and eastern margins. Recent numerical modelling simulations have suggested that this ice sheet sector underwent a period of rapid thinning during the Bølling–Allerød warm period and likely contributed to rapid sea level rise during this time (Gregoire et al., 2016). But sparse empirical constraints on the timing and pattern of retreat make it difficult to verify whether this rapid retreat occurred. As such, this ice sheet sector presents a clear opportunity to investigate the dynamics of ice

sheet retreat during climatic oscillations following the end of the LGM and test the validity of ice sheet modelling results.

## 1.1 Glacial history of the Laurentide Ice Sheet:

In this section, I will provide a brief overview of the glacial history of the LIS throughout the Quaternary, with a focus on the northwestern sector.

### 1.1.1 Pre-LGM understanding:

A multi-dome LIS first occurred at the start of the Quaternary, during the Matuyama chron (~2.6 – 1.8 Ma; Balco and Rovey, 2010; Barendregt and Duk-Rodkin, 2011; Batchelor et al., 2019; Evans et al., 2021). Before this time, continental ice in Northern America likely consisted of two independent ice domes of limited extent over Labrador and Keewatin (Barendregt and Duk-Rodkin, 2011; Batchelor et al., 2019). Early reconstructions suggested the ice dome situated over Labrador extended as far south as 39°N but was unconnected to ice in the Keewatin region (Barendregt and Duk-Rodkin, 2011). In the Keewatin region, local ice caps were suggested as the dominant glaciation style (Barendregt and Duk-Rodkin, 2011). However, a recent re-examination of the glacial stratigraphy has suggested that the local ice cap hypothesis is unfounded and constrains the first advance of a Keewatin Ice Dome over northwestern Canada to 2.9±0.3Ma using cosmogenic nuclide burial dating (Evans et al., 2021) at broadly the same time as Labrador ice reached 39°N (2.4±0.14 Ma; Balco and Rovey, 2010). Together, these constraints support the idea of an early large LIS which may have been facilitated by a deformable regolith of preglacial material (Clark and Pollard, 1998; Balco and Rovey, 2010; Batchelor et al., 2019; Evans et al., 2021).

The LIS did not reach a similar size to this first advance until the Late Matuyama (Balco and Rovey, 2010). The next appearance of the LIS in the US at 39°N occurred as late as 1.3±0.09Ma, according to cosmogenic nuclide burial ages, with three more advances occurring between 0.79±0.1Ma and 0.22±0.16Ma (Balco and Rovey, 2010). This represents a change to more extensive LIS glaciations following the mid-Pleistocene transition. However, there are no comparable records of glaciation for the northwestern sector of the Laurentide Ice Sheet and the uncertainty bounds in the reconstruction of Batchelor et al. (2019) are large. In fact, there is currently no evidence that the LIS extended west of the modern-day Mackenzie River at any time prior to the LGM (Duk-Rodkin et al., 1996; Duk-Rodkin and Barendregt, 2011).

The last glacial cycle (~115 ka to ~10 ka) is comparatively better constrained than the oldest Quaternary glaciations of North America, but significant uncertainties remain in the MIS 3 (57 – 29 ka) ice sheet extent. A recent review of this period by Dalton et al. (2022) highlighted multiple cycles of build-up and decay during this time. The Keewatin Ice Dome first reappeared at ~75 ka and contributed to the peak in ice extent at ~60 ka, which almost matched the all-time maximum extent (Dalton et al., 2022). This was followed by a significant reduction in ice at ~45 ka, although key uncertainties remain regarding whether Hudson Bay was ice-free between 50 and 40 ka. Arguments for an ice-free Hudson Bay are supported by luminescence and radiocarbon ages (Dalton et al., 2016; Pico et al., 2017; Dalton et al., 2019), while arguments for glaciation often question the reliability of these ages and the necessity of a glaciated Hudson Bay to produce Heinrich Events 4 and 5 (Miller and Andrews, 2019; Hodder et al., 2023). Regardless of whether Hudson Bay remained glaciated between 50 and 40 ka, the LIS began a gradual growth to its maximum extent following this period.

### 1.1.2 The LGM ice sheet configuration:

The LIS reached its all-time maximum extent during the last glaciation with a global mean sea level equivalent volume of between 49.4 – 55.8 m (Licciardi *et al.,* 1998; Clark and Mix, 2002; Dyke *et al.,* 2002). The spatial extent has been well-constrained by numerous surficial geological mapping campaigns from the Geological Survey of Canada for the onshore record (Dyke and Prest, 1987; Fulton, 1995). The offshore ice limits on the continental shelf are much less certain, but at the marine-terminating eastern and northern margins it likely extended to the continental shelf break and the southern margin extended as far as 38°N in the US (Dalton et al., 2023). In the north, it was coalesced

with the Innuitian Ice Sheet and the western margin was located along the range front of the Canadian Cordillera and coalesced with the Cordilleran ice sheet between ~65°N to ~48°N (Dalton et al., 2023; Figure 1).

The maximum extent of the LIS was asynchronous, with as much as 10,000 years difference between the local LGM of different ice sheet sectors (Dalton et al., 2020; Dalton et al., 2023). The southern margin may have reached its maximum position as early 27 ka (Curry et al., 2018). An early maximum extent has also been proposed for the marine-terminating eastern margin, although this has yet to be confirmed by numerical dating methods (Dalton et al., 2023). The early advance to the maximum extent in these sectors is likely due to the close proximity of the ice source area to the continental shelf break, which provided a limit on the extent on the eastern margin.

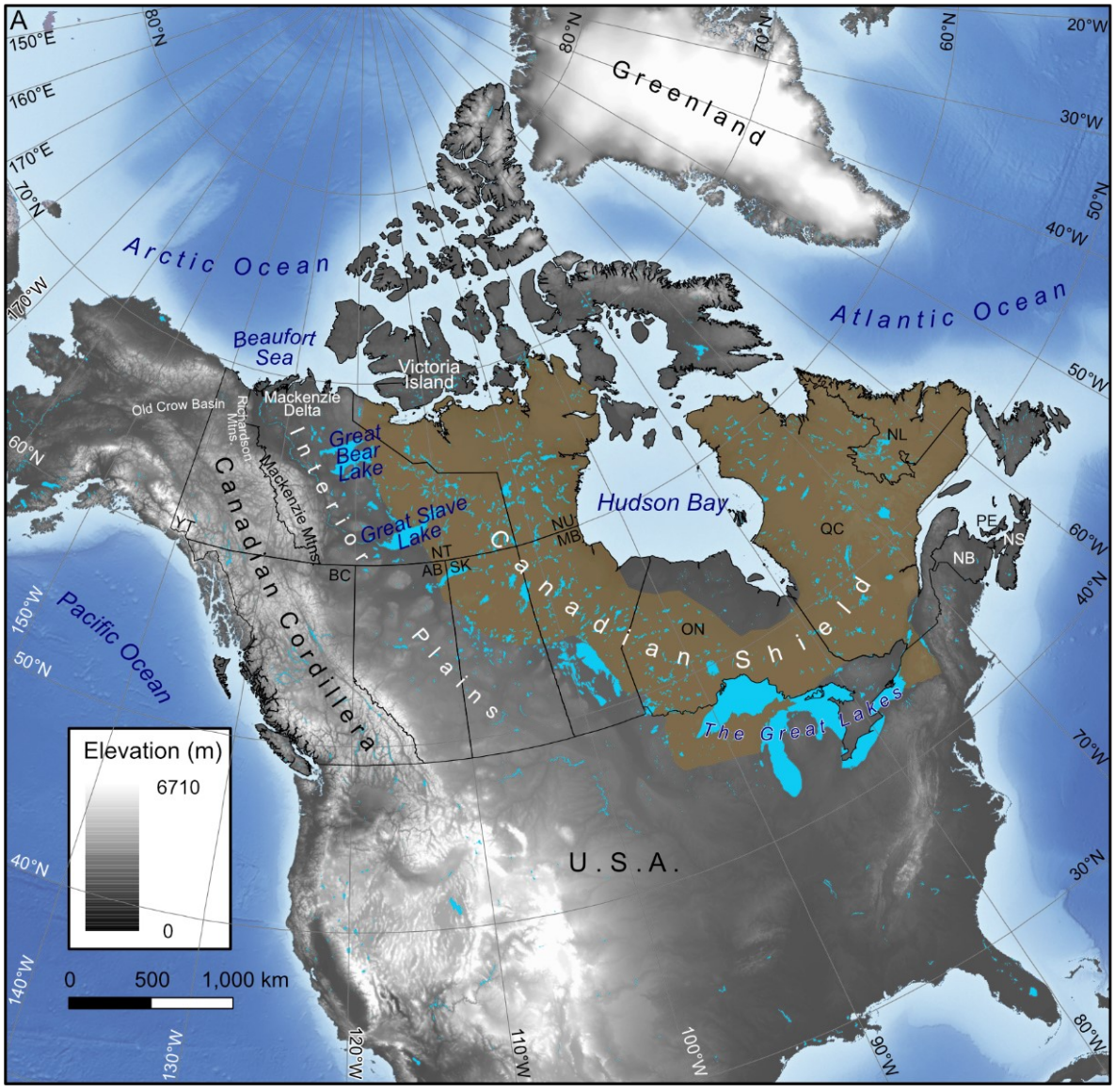


Figure 1A: Topographic map of North America of the key physiographic regions studied in this thesis.

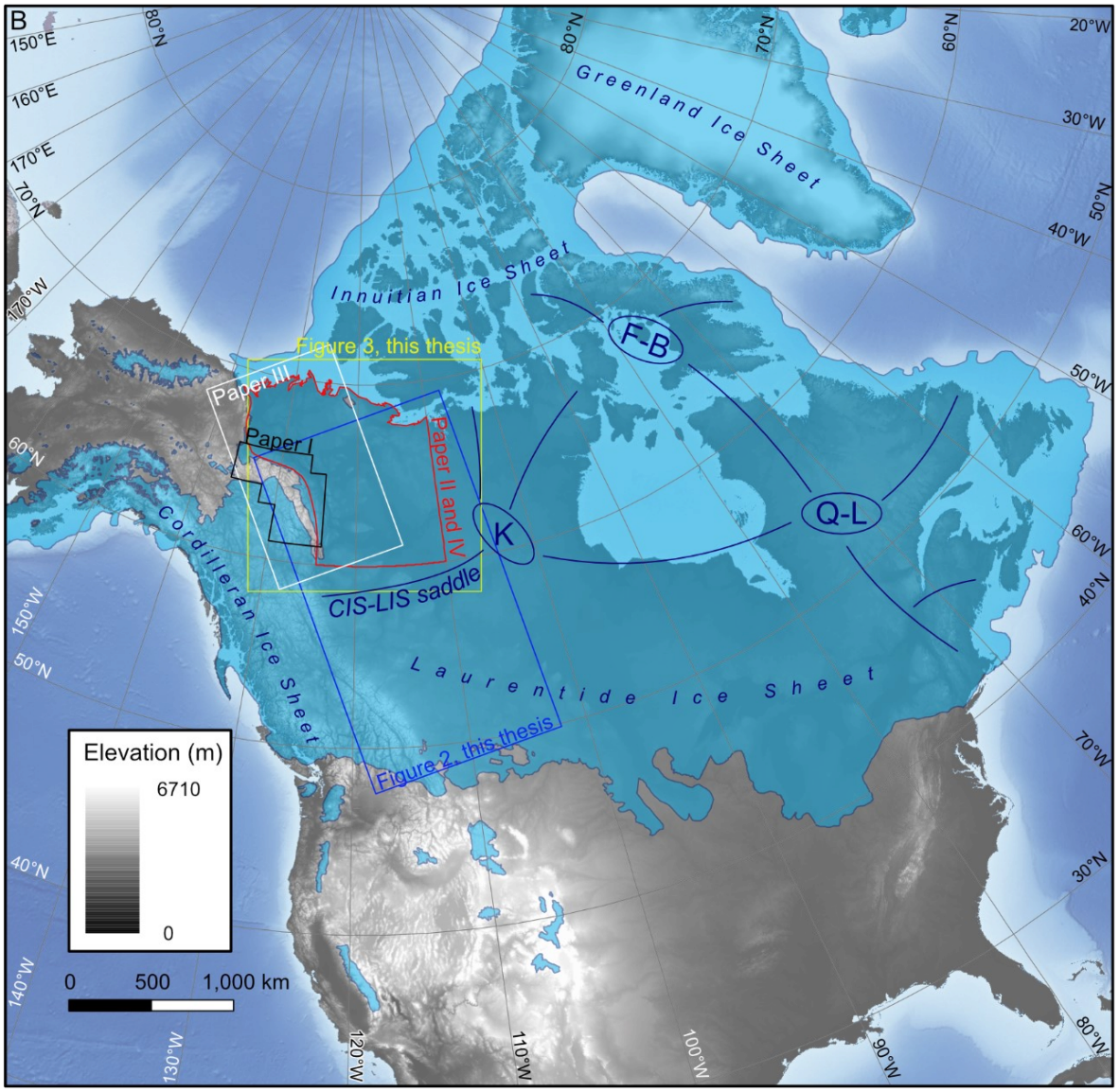


Figure 1B: The extent of the North American Ice Sheet Complex during the Last Glacial Maximum at 18.0 ka $^{14}$C /21.1 ka cal. BP (Dalton et al., 2020). The approximate location of ice domes (dark blue ovals) and ice divides (dark blue lines) are reproduced from Margold et al. (2018). The study area of each paper and the figure locations in this thesis are indicated by the coloured boxes.

During the advance to its local LGM, the Keewatin dome of the LIS advanced west over the Interior Plains towards the Canadian Cordillera (Kleman et al., 2010; Margold et al., 2018). As the LIS reached the Cordillera it coalesced with the Cordilleran Ice Sheet for the first time in the Quaternary (Batchelor et al., 2019). The coalescence of the ice sheets led to the formation of the Cordilleran-Laurentide ice saddle which caused the northwards deflection of ice flow north of ~60°N and the southwards deflection of ice flow to the south of ~60°N (Margold et al., 2018). Northerly deflected ice flowed down the Mackenzie Valley towards the maximum extent position. Early reconstructions placed the ice limits at the Sitidgi Stade moraines, suggesting that the LIS did not extend significantly offshore (Rampton, 1988). However, marine geophysical surveys have confirmed that the ice sheet extended to the continental shelf break during the last glaciation (Batchelor et al., 2013, 2014). Combined with surficial geological mapping from the Geological Survey of Canada, the glacial limits of the northwestern LIS are well constrained, although considerable uncertainties remain in the timing of the local LGM (Duk-Rodkin, 1999, 2022).

During the 1980s and 1990s, the glacial lake records from the unglaciated regions of the Yukon, beyond the Richardson Mountains, were used to constrain the maximum extent of the northwestern LIS (Catto,

1986; Morlan et al., 1990; Lemmen et al., 1994; Duk-Rodkin and Hughes, 1995). As the LIS advanced to the front of the Richardson Mountains, it dammed the eastwards drainage from the Yukon and led to the development of glacial lake Old Crow (Kennedy et al., 2010). Radiocarbon ages were used to suggest an early local LGM of the LIS at ~30 ka, followed by a readvance at ~22 ka (Duk-Rodkin and Hughes, 1991; Duk-Rodkin et al., 1996; Zazula et al., 2004). A series of early $^{36}$Cl cosmogenic nuclide exposure ages were also used to support this interpretation but were never published in full and include large uncertainties (Duk-Rodkin et al., 1996). The cross-cutting of montane glacier moraines by LIS meltwater channels was thought to require a readvance of the LIS that would support this chronology, but this interpretation does not account for the possibility of non-erosive, cold-based ice (Duk-Rodkin and Hughes, 1991).

An alternate chronology has been proposed whereby the local LGM of the northwestern LIS occurred much later and was relatively short-lived (Kennedy et al., 2010; Murton et al., 2015). A realisation of the high preservation potential of woody material and pine needles in Arctic settings necessitated a re-evaluation of the radiocarbon ages constraining the deglacial sequence (Kennedy et al., 2010). Many of the pre-existing ages represent non-finite, reworked material that does not relate to the LGM and should be disregarded (Kennedy et al., 2010). Radiocarbon dating of low preservation potential material suggests that the maximum extent occurred sometime after ~19.1 ka cal BP (18.9–19.4 ka cal BP) (Kennedy et al., 2010) and is supported by luminescence ages on pre- and post-glacial dune sands from the Mackenzie Delta suggesting a short-lived maximum sometime between 17.5 ka and 15 ka (Murton et al., 2015). A late local LGM for the northwestern LIS is logical as the large geographical distance from the Keewatin Ice Dome to the continental shelf in the Beaufort Sea would require a long build-up phase. The advance to the maximum extent also likely only occurred following the formation of the ice saddle which occurred sometime after ~25 ka (Heintzman et al., 2016). However, pre- and post-glacial luminescence ages are often overlapping meaning that many uncertainties remain around the precise timing and duration of the local LGM.

### 1.1.3 The last deglaciation:

The last glacial termination was characterised by millennial-scale climate oscillations that drove changes in global ice volume (Broecker et al., 1989; Yu and Wright Jr., 2001; Clark et al., 2002). The Bølling–Allerød interstadial (14.7 – 12.9 ka) was a period of rapid warming in the Northern Hemisphere associated with enhanced rates of deglaciation and rapid sea level rise (Deschamps et al., 2012; Buizert et al., 2014). In North America, the Cordilleran Ice Sheet lost up to half of its mass over 500 years during the Bølling–Allerød (Menounos et al., 2017) with similar trends of accelerated ice mass loss observed for the LIS (Wickert et al., 2013; Barth et al., 2019). The overall trend of deglaciation was interrupted by a climatic reversal during the Younger Dryas stadial (12.9 – 11.7 ka) when falling temperatures led to the stabilisation or readvance of ice masses (Buizert et al., 2014). The regional strength of these millennial-scale climate changes across the Northern Hemisphere and the response of ice sheets to these climate events is varied (Alley, 2000; Fastovich et al., 2020; Fastovich et al., 2022).

In the ice margin chronology of Dalton et al. (2020; Figure 2A), which is simply a recalibration of the Dyke et al. (2003) reconstruction for this ice sheet sector, the northwestern LIS retreat does not appear to be driven by these climatic events. During the Bølling–Allerød, ice margin retreat rates were low at ~66 m/year, as the ice margin remained near the modern-day coastline (Dalton et al., 2020). The ice margin retreat rates rapidly increased to ~333 m/year as the ice margin retreated across the Northern Interior Plains throughout the Younger Dryas (Dalton et al., 2020) and remained high (466 m/year) for the following 1,500 years as the ice margin retreated to the Canadian Shield by 10 ka. Ice margin retreat rates only decreased after 10 ka, when the LIS margin stabilised on the Canadian Shield (Dalton et al., 2020). This ice margin retreat sequence conflicts with the expected ice sheet response to the Bølling–Allerød and Younger Dryas climate oscillations. In contrast to the northwestern sector, the southwestern LIS underwent a period of rapid retreat during the Bølling–Allerød followed by ice margin stabilisation during the Younger Dryas cooling (Norris et al., 2022).

Recent numerical modelling studies have suggested that the northwestern LIS might have experienced a period of rapid thinning during the Bølling–Allerød and contributed to rapid sea level rise events

(Gregoire et al., 2012, 2016; Gomez et al., 2015; Ivanovic et al., 2017). Rising temperatures during the Bølling–Allerød are hypothesised to have caused a negative surface mass balance in the ice saddle region leading to ice sheet surface lowering (Gregoire et al., 2012, 2016). As the ice saddle thinned, the ice sheet surface reached progressively lower elevations and was exposed to warmer temperatures which enhanced melt rates and caused an elevation-melt feedback and the rapid collapse of the ice saddle (Gregoire et al., 2012). However, the paucity of constraints on deglaciation in this region make it difficult to verify these modelling results.

## 1.2 Motivation:

Providing new empirical constraints on the timing, extent and retreat dynamics of the northwestern LIS is the key motivation of this thesis. These empirical constraints will be used to develop a reconstruction of the chronology and dynamics of ice sheet retreat that can be used to validate numerical modelling simulations and gain an insight into the drivers of ice sheet retreat. The high-resolution digital elevation model ArcticDEM (2 m resolution) provides an opportunity to map large areas of the former ice sheet bed in a time-efficient manner for large, remote regions. We use the ArcticDEM to create detailed maps of the glacial geomorphology of the majority of the Northwest Territories (paper I and II).

Prior to this thesis, the chronology of the northwestern LIS was only loosely anchored by a small number of radiocarbon dates that only provided a minimum age constraint on the timing of deglaciation. This limited our ability to understand the drivers of ice sheet retreat and calculate the contribution to past sea level rise. In paper II, we provided new cosmogenic nuclide exposure age constraints on deglaciation to revise the ice margin chronology for the region and identify a period of rapid deglaciation during the Bølling–Allerød. Finally, we combine our reconstruction with numerical modelling simulations to quantify the contribution to GMSL during the last deglaciation from this ice sheet sector.

There is no previously published ice flow reconstruction for the northwestern LIS, which limits our ability to understand the drivers of periods of rapid ice margin retreat or stabilisation. Within paper IV, we sought to leverage the geomorphological record (mapped in paper II) and a newly published ice margin chronology (Dalton et al., 2023; that was largely based on the interpretations presented in paper III) to investigate the dynamics of the ice drainage network and the nature of the ice margin retreat processes. The retreat of the northwestern LIS spans the Bølling–Allerød and Younger Dryas climate oscillations that followed the LGM and allows us to investigate the response of ice flow dynamics to millennial-scale climatic changes.

## 1.3 Objectives:

The aim of this thesis is to build an empirical reconstruction of the deglaciation of the northwestern LIS to investigate the response of ice sheets to climate change, the drivers of ice sheet change and the implications for past changes in sea level. To accomplish these aims we followed these objectives:

1. To create a map of the glacial geomorphology of the northwestern LIS (paper I and II).
2. To provide age constraints on the rate of ice sheet retreat and thinning by combining new cosmogenic nuclide exposure age constraints and pre-existing chronological constraints (paper III).
3. To apply the glacial inversion method and flowset mapping approach to reconstruct the ice flow dynamics and margin retreat processes of the northwestern LIS (paper IV).

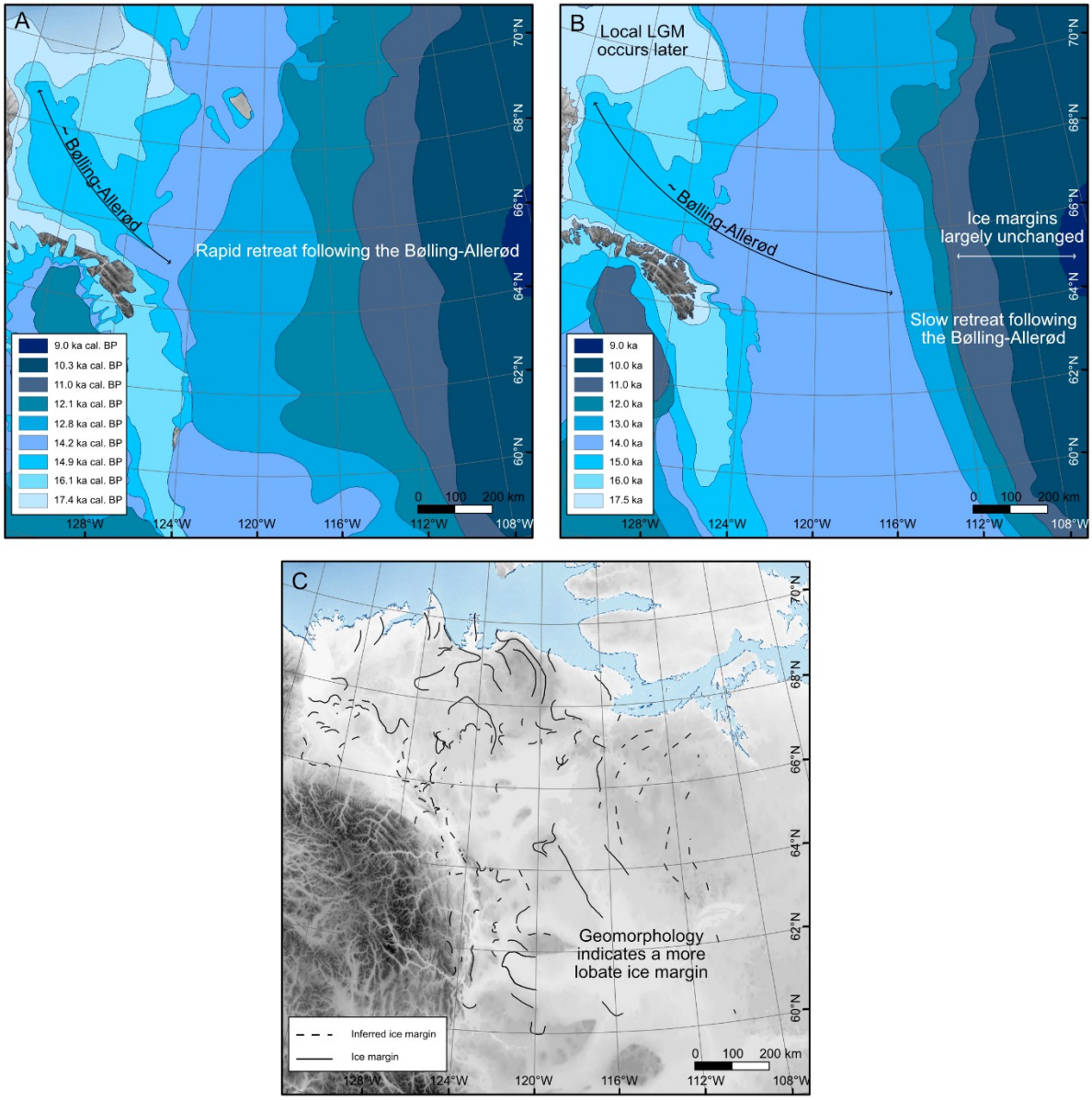


Figure 2: The development of the ice margin chronology and retreat pattern for the northwestern LIS. (A) The radiocarbon-based ice margin chronology of Dalton et al. (2020), which is largely a recalibration of the Dyke et al. (2003) ice margins for this ice sheet sector. (B) The ice margin chronology of Dalton et al. (2023), which is anchored by the exposure ages presented in paper III. The youngest ice margins, in the east, are largely unchanged from the previous ice margin chronology due to the absence of any new constraints. (C) The ice margin retreat pattern from paper IV that has not been constrained by any temporal framework. Note how our ice margin retreat pattern indicates more lobate ice margins and provides much greater detail than the broad-scale isochrones.

# 2.0 Study area:

This doctoral dissertation is focused on the northwestern sector of the LIS. During the last glaciation, the northwestern sector of the LIS extended along the range front of the northern Canadian Cordillera and subsumed the foothills of the Mackenzie Mountains in the Northwest Territories (Figure 1A and B; Dalton et al., 2023). It extended up the valleys of the Mackenzie Mountains, where it coalesced with local montane glaciers. Over the southern Mackenzie Mountains, it merged with the Cordilleran Ice Sheet to form the Cordilleran-Laurentide ice saddle. In the north, the margin was marine-terminating and extended to the continental shelf edge and was merged with the Innuitian Ice Sheet over the Canadian Arctic Archipelago.

While the thesis is concerned with the broader northwestern LIS, the study area extent for each chapter is different. Paper I covers the Mackenzie Mountains region and paper II covers the Northern Interior Plains and Canadian Shield to 110°W, meaning that these two glacial geomorphological maps provide near-complete coverage of the former bed of the northwestern LIS. Paper III is much narrower in geographical scope and is focused on the central Mackenzie Valley region, and paper IV covers the Northern Interior Plains and western Canadian Shield region. The locations mentioned in this thesis are indicated on Figure 1A and the extent of each study is indicated in Figure 1B.

## 2.1 Topographic setting:

The study area spans three distinct physiographic regions: the Mackenzie Mountains in the west, the Northern Interior Plains in the centre, and the Canadian Shield in the east. It extends from 60°N to the present-day coastline.

The Mackenzie Mountains and their foothills form part of the northern Canadian Cordillera, extending over 500 km in length and over 150 km wide. To the west of the Mackenzie River, the Canadian Cordillera can be separated into two northerly-trending mountain ranges, including the Backbone Ranges on the west and the Canyon Ranges on the east. The Backbone Ranges form the interior of the Mackenzie Mountains and are characterised by high peaks up to 2,400 m in elevation and a topography which has been significantly modified through multiple glacial cycles (Duk-Rodkin and Hughes, 1992), with the highest peaks still holding small cirque glaciers (Hawkins et al., 2023). To the east of the Mackenzie River, the Franklin Mountains is a small range of low peaks (<1,600 m) that delineate the eastern boundary of the Cordillera.

The Northern Interior Plains extend from the eastern flank of the Mackenzie Mountains to the western edge of the Canadian Shield and can be separated into seven separate subdivisions: the Horton Plain, Anderson Plain, Colville Hills, Peel Plain, Mackenzie Plain, Great Bear Plain, and Great Slave Plain. These plains can occupy both lowland (e.g. Mackenzie Plain at ~200 m elevation) or upland positions (e.g. the Horton Plain at ~500 m elevation) but are typically low relief areas. The Northern Interior Plains are characterised by soft bedrock and a thick drift cover of glacial till that was deposited during the last glaciation (Fulton, 1995; Smith et al., 2023).

The Canadian Shield is the easternmost physiographic region covered in this thesis and comprises a broad region of low relief, exposed Precambrian igneous rock with widespread surface exposures (Figure 1A). In contrast to the Northern Interior Plains, surficial drift cover is limited and where present is often only a thin veneer of till cover as repeated glaciations eroded any surficial cover (Fulton et al., 1995). The Canadian Shield extends from the Great Lakes at ~46°N in the south to the contemporary coastline with the Arctic Ocean in the north. While the Canadian Shield spans as far east as 56°W, our study area only extends to 110°W and north of 60°N.

## 2.2 Climate:

The former bed of the northwestern LIS covers >1,000,000 $km^2$ and exhibits spatial and temporal climatic variability, but can be broadly characterised as subarctic with cold, dry winters and short, mild summers (Phillips 1990; Peel et al., 2007). Based on climate normals for Norman Wells, the average winter daily minimum temperature is -30°C with extreme minimum temperatures as low as -52°C in

January. In the summer, temperatures of up to 35°C have been recorded but average summer daily temperatures of between ~11°C and ~22°C are more common (Government of Canada, 2023). Annual precipitation is typically low, with an annual average of <300 mm/year. Around half of all precipitation occurs as rainfall between May and September, and the other half as snowfall between September and May (Government of Canada, 2023). Surface snow cover is common from October to April with maximum depths of up to 30 cm (Government of Canada, 2023). Precipitation values are highest in the Cordillera region and decrease to the east due to the rain shadow effect, with a further trend of decreasing precipitation to the north (Phillips, 1990; Bailey et al., 1997; Persaud, 2023). These climatic conditions have contributed to the development of large thicknesses of permafrost and ground ice (Burn, 1994). Ground ice was predominantly formed in the Late Wisconsinan and includes buried glacial ice from the last glaciation (Burn, 1994; Murton et al., 2004; 2005).

## 2.3 Permafrost distribution:

Our study area spans a high latitudinal range and crosses multiple different permafrost zones. The southernmost portion of the study area, around the Great Slave Lake at ~60°N – 62°N, is situated in the sporadic discontinuous permafrost zone (Hegginbottom et al., 1995). Between ~62°N – 65°N can be characterised as extensive discontinuous permafrost and north of ~65°N is the continuous permafrost zone. There is also a south to north gradient in the ground ice conditions, with the highest ground ice content observed around the Mackenzie Delta region (~70°N) and decreases to the south. Compared to similar latitudes, ground ice content in the Northern Interior Plains is generally higher than in the adjacent Mackenzie Mountains or on the Canadian Shield (Hegginbottom et al., 1995). Contemporary climate change and rising temperatures mean that these landscapes are currently undergoing dramatic changes due to the widespread thaw of permafrost (Kokelj et al., 2017).

# 3.0 Data and methods

## 3.1 Geomorphological mapping

Papers I and II present maps of the glacial geomorphology of the bed of the former northwestern LIS. In paper I, the study area was focused on the broader Mackenzie Mountains region and intended to cover the area glaciated by the LIS, Cordilleran Ice Sheet and the local montane glaciations so that the interactions between these ice masses could be investigated. In paper II, the map extent was bounded by the 60$^{th}$ parallel in the south due to the availability of the high-resolution ArcticDEM data and in the north was bounded by the present-day coastline. The northern Canadian Cordillera marked the western boundary and 110°W is the eastern boundary.

The glacial geomorphological mapping was undertaken using a repeat-pass method with a hillshaded elevation model (ArcticDEM, 2 m resolution; Porter et al., 2018) and landform identification was based on their morphology, spatial distribution, and relationship with surrounding landforms (Chandler et al., 2018). The Image Mosaic of Canada v1 with a 30 m resolution (Government of Canada, 2013) and PlanetLabs imagery with a 2 m resolution were used to supplement the ArcticDEM in places of lower data quality or blank spots.

## 3.2 Terrestrial Cosmogenic Nuclide (TCN) exposure dating

### 3.2.1 The fundamentals of TCN accumulation at the Earth's surface

High energy cosmic particles generated by supernova explosions collide with atoms in the upper atmosphere, leading to a cascade of reactions that produces secondary particles that can collide with target atoms and produce cosmogenic nuclides in the atmosphere or on the Earth's surface (Dunai and Lifton, 2014; Ivy-Ochs and Briner, 2014). These cosmogenic nuclides ($^{3}$He, $^{10}$Be, $^{14}$C, $^{21}$Ne, $^{26}$Al, $^{36}$Cl) are rarely, naturally produced at the Earth's surface, with 98% of cosmogenic nuclides production occurring due to these secondary cosmic ray particles in the upper few metres of rock (Dunai and Lifton, 2014). The rate of cosmogenic nuclide production is heavily dependent on the intensity of the cosmic ray flux which varies across the globe (Ivy-Ochs and Briner, 2014; Schaefer et al., 2022). At high latitudes, the pathway of cosmic rays is roughly subparallel to the magnetic field lines and few particles are blocked from reaching the surface. At lower latitudes, the perpendicular pathway of cosmic rays relative to the magnetic field lines means that large proportions of the flux may be blocked. In addition to this, elevation is a strong control on the cosmic ray flux reaching the surface as cosmic rays travelling to higher elevation surfaces travel through a smaller distance of the atmosphere and less cosmic rays are blocked compared to lower elevation surfaces (Desilets and Zreda, 2001).

TCN exposure dating is principally concerned with the in-situ production of these rare nuclides in rocks at the Earth's surface and leverages their accumulation to quantify the amount of time that a surface has been exposed to cosmic rays. In paper III, we apply the method of TCN exposure dating using $^{10}$Be to constrain the timing of deglaciation for the northwestern LIS.

### 3.2.2 Sample site and boulder selection

Since the early 1990s, TCN exposure dating has been applied to constrain the timing of deglaciation across the world (Phillips et al., 1994; Jackson et al., 1997; Balco, 2011; Ivy-Ochs and Briner, 2014). Various sampling site selection strategies exist and can include the targeting of glacial landforms, including moraines to constrain ice margin standstills (Applegate et al., 2010; Ivy-Ochs and Briner, 2014). Alternatively, erratics from formerly glaciated areas that are not associated with a particular landform can be sampled to simply constrain the timing of ice-free conditions (von Blanckenburg and Willenbring, 2014). Sampling may also occur along transects to constrain the rate of deglaciation. Studies which seek to constrain the rate of ice margin retreat can sample along a horizontal transect (Jones et al., 2019). Alternatively, in mountainous regions, the ice sheet thinning rate can be constrained through sampling surfaces along an elevation transect (Small et al., 2019; Halsted et al., 2023). In paper III, we selected our sample locations across a range of different elevations, latitudes and longitudes to constrain both the thinning rate and ice margin retreat pattern. Regardless of the sampling strategy, all

sampling for TCN exposure dating should be well-contextualised by detailed mapping of the geomorphological context of a site.

The practice of TCN exposure dating relies upon two assumptions that guide the field sampling procedure: 1) the sampled surface is fresh and has not previously been exposed to cosmic rays prior to its exposure during deglaciation and 2) following deglaciation, the sampled surface has experienced continuous exposure with no shielding from cosmic rays (Heyman et al., 2011; Ivy-Ochs and Briner, 2014). Anomalously old exposure ages might occur when the first assumption is not valid and this occurs when a sampled surface has not experienced enough erosion to 'reset' the cosmogenic signal that was developed prior to deposition, with a couple of metres of erosion typically required for this (Balco, 2011). As such, we attempted to sample from erratics which were subrounded in shape, as this may suggest that the boulder has had a longer transport history than more angular boulders. In contrast, if a sample has experienced an incomplete exposure due to post-depositional shielding from cosmic rays, then the exposure age would be anomalously young (Balco, 2011). A range of factors can lead to incomplete exposure of a surface and sampling strategies should select boulders to mitigate these risks. For example, a boulder deposited on an unstable slope may have slumped or rolled following deposition and so it is preferable to sample boulders situated on a stable surface (e.g on bedrock) and not near the base of steep slopes. Surfaces may also be partially shielded from cosmic rays by the surrounding topography, snow cover and/or vegetation and corrections can be applied to account for this (Gosse and Phillips, 2001).

### 3.2.3 The extraction of cosmogenic nuclides from rock samples

The target mineral must be separated from the collected samples to allow the concentration of the target cosmogenic nuclide to be measured. In paper III, we extracted quartz from granitoid samples to allow the amount of $^{10}$Be to be quantified. This involves the crushing and grinding rock samples to attain a grain size of 125–500μm and a series of steps to isolate the pure quartz which can involve a range of steps including: magnetic separation, froth floatation to remove feldspars, and leaching in hot hydrofluoric acid (Schaefer et al., 2022). The pure quartz sample must then be spiked with a carrier of $^{9}$Be before being digested in a HF-$HNO_3$ mixture and treated with anion and cation column chemistry to isolate Be2+ which can eventually be packed into stainless steel cathodes for analysis at the AMS to determine the quantity of $^{10}$Be.

### 3.2.4 Exposure age calculation approach

The calculation of exposure ages from the measured $^{10}$Be concentrations then requires: a production rate, a scaling model, and any necessary corrections. There are currently no established best practice guidelines, and each study must consider the characteristics of their sampled sites to make the most appropriate choices.

The production rate is the rate at which cosmogenic nuclides are produced in a mineral at a specific site. There are many production rate calibration datasets and the most popular for studies of North American glaciations are: the global production rate (based on the primary calibration data set; Borchers et al., 2016), Arctic production rate (based on the Baffin Bay calibration dataset; Young et al., 2013), and the Northeast North America (NENA) calibration data set (Balco et al., 2009). Each calibration data set spans a specific range of elevations, latitudes, times and settings which make them most appropriate in separate regions. A previous study of the northwestern LIS used the Arctic production rate when calculating the exposure age of samples on the Canadian Shield (Reyes et al., 2022). While this choice was appropriate for their sites, our sites are located above the recommended elevation range for the use of the Arctic production rate (1,000 m; Young et al., 2013). Therefore, in paper III, we calculate our exposure ages using the global production rate (Borchers et al., 2016).

As previously described, the flux of cosmic rays varies spatially so a scaling model must be applied to the known production rate to adjust for the changes in elevation and latitude between the production rate site and the sampled sites. The selection of different scaling methods has a minimal (~2%) effect on the calculated exposure age. We opt to use the time-dependent LSDn scaling model in paper III (Lifton et al., 2014).

In paper III, we discuss the implications of different corrections for TCN exposure age calculation. The subarctic, low precipitation conditions of our sampling sites mean that shielding by snow and vegetation cover was likely negligible for the sampled boulders (Schildgen et al., 2005; Plug et al., 2007). The granitoid lithology of sampled boulders, dry continental climate and lack of vegetation on the surfaces means that we assume surface weathering was limited. We therefore apply no correction for these processes. However, we do apply a correction for the change in elevation of the sample sites due to glacial isostatic adjustment (GIA) of the landscape, which makes our ages between 0.1% and 3.5% older, depending on the site. The effect of changes in the atmospheric conditions following deglaciation has been suggested to offset the influence of GIA on exposure age calculations (Staiger et al., 2007), however, multiple studies have suggested that the influence of atmospheric changes is an order of magnitude lower than the influence of GIA changes (Cuzzone et al., 2016; Dulfer et al., 2021), so we opt not to apply a correction for atmospheric changes.

To ensure comparability between our sites and those in the surrounding regions, in paper III, we recalculate pre-existing exposure ages to create an internally consistent dataset. In the discussion section of this thesis we provide a more detailed discussion of the implications and importance of exposure age calculation approaches.

## 3.3 Glacial inversion method and flowset mapping

In paper IV, we follow the established glacial inversion methodology to use the spatial distribution of glacial landforms (presented in paper II) to reconstruct the ice margin retreat pattern of the northwestern LIS (Kleman and Borgstrom, 1996; Clark, 1997; Greenwood et al., 2007). Across the Northern Interior Plains, moraines are widespread and provide relatively detailed information on the ice margin configuration. On the Canadian Shield, moraines are largely absent and the ice margin retreat pattern is predominantly derived by extrapolation between eskers based on the assumption that they formed perpendicular to the ice margin. The morphology of these landforms is investigated to provide an insight into the ice margin retreat processes (Evans et al., 1999; Dyke and Evans, 2014).

The mapped glacial lineations are grouped into flowsets, which are coherent patterns of lineations that share a similar morphology and orientation. The cross-cutting relationships and overprinting of these flowsets is then used to reconstruct the relative sequence of ice flow events (Greenwood and Clark, 2009). These flow events are then constrained in time by the ice margin chronology of Dalton et al. (2023) to create an ice flow reconstruction at 500-year timesteps throughout the last deglaciation.

Flowsets are placed into four separate categories based on: lineation morphology, the association with deglacial landforms, and the degree of topographic influence on the lineation orientation. Ice stream flowsets are identified by the highly elongated lineations that comprise them and indicate tracts of fast ice flow. The remaining flowsets are all interpreted to have formed during a slower ice flow regime. Event flowsets formed towards the interior of the ice mass and are identified by the high parallel conformity of lineations, lack of association with deglacial features, and the fact that they are commonly fragmented in appearance. Deglacial and deglacial inferred flowsets formed near to the ice sheet margin. Deglacial flowsets are identified by the association with deglacial landforms (e.g. moraines and eskers), while deglacial inferred flowsets are identified based on the strong influence of topography on lineation pattern or diverging lobate lineation patterns that suggest formation near the ice sheet margin (Hughes et al., 2014).

# 4.0 Overview of publications

## 4.1 Paper I

Stoker, B.J., Margold, M. and Froese, D., 2023. The glacial geomorphology of the Mackenzie Mountains region, Canada. *Journal of Maps*, pp.1-12

In this paper, I present a map of the glacial geomorphology of the broader Mackenzie Mountains region, Canada. The map stretches from 61°N to 66°N and covers the Canyon and Backbone ranges of the Mackenzie Mountains. In the east, it includes part of the Mackenzie Mountain foothills and in the west, it includes part of the Selwyn Mountains. A total of 21 1:250,000 National Topographic System (NTS) map sheet areas were covered, of which 8 were previously unmapped. The glacial geomorphology was primarily classified using the ArcticDEM elevation dataset (2 m resolution; Porter et al., 2018), with PlanetLabs satellite imagery used to cover the blank spots in the ArcticDEM.

Glacial lineations are the largest landform category, with 11,795 mapped. There are clear spatial trends in the distribution and morphology of glacial lineations. The majority of glacial lineations are observed at low elevations along valley floors and almost half of the mapped glacial lineations are located in the Mackenzie Valley. The lineations in the Mackenzie Valley also displayed a more elongate morphology than those in the Mackenzie Mountains.

Meltwater channels are classified into three separate categories: lateral meltwater channels ($n$=9766), undifferentiated meltwater channels ($n$=985), and lateral meltwater spillways ($n$=72). Lateral meltwater channels are further divided into three subcategories relating to the ice source they are formed by: montane, Cordilleran, or Laurentide. The majority of lateral meltwater channels were formed by the retreat of ice lobes from the Cordilleran Ice Sheet in the western Mackenzie Mountains, although some examples relating to the LIS along the eastern Mackenzie Mountains are observed. In contrast, lateral meltwater spillways are located exclusively along the eastern range front of the Mackenzie Mountains with a south-north orientation and were likely formed during the drainage of glacial lakes that were impounded between the LIS margin and the mountains (Bednarski, 2008; Huntley et al., 2017).

Moraines are widespread across the Mackenzie Mountains and mark the extent and retreat patterns of the Cordilleran and Laurentide ice sheets and montane ice masses. Similar to lateral meltwater channels, we include three subcategories of moraine related to the ice mass it was formed by: montane, Cordilleran or Laurentide. Across the Mackenzie Mountains, we observe multiple instances of cross-cutting relationships whereby montane moraines have been cross-cut by meltwater channels from either the Cordilleran or Laurentide ice sheet and this provides an insight into the relative timing of ice advances.

Eskers are the final landform category and provide an indication of the former ice retreat patterns. Eskers trend along the valley floor and appear to record the retreat of ice lobes along the valleys of the Mackenzie Mountains. Examples of eskers on upland plateaus are much less common.

The glacial geomorphological record across the Mackenzie Mountains is highly varied, with each ice source exhibiting its own distinct signature. The geomorphological map holds key information to allow the reconstruction of the maximum extent and retreat patterns of the montane, Cordilleran and Laurentide ice masses, while the cross-cutting relationships record the relative dynamics and interactions between these ice masses.

## 4.2 Paper II

Dulfer, H.E., Stoker, B.J., Margold, M. and Stokes, C.R., 2023. Glacial geomorphology of the northwest Laurentide Ice Sheet on the northern Interior Plains and western Canadian Shield, Canada. *Journal of Maps*, pp.1-18

In this paper, we present a map of the glacial geomorphology of the former bed of the northwestern LIS. The southern extent of the map is set to 60°N and is defined by the limit of ArcticDEM data availability and the northern mapping limit of other studies (Norris et al., 2017, 2023) and extends to the modern-day coastline in the north. The western extent is set along the eastern edge of the Canadian Cordillera and extends to 110°W to capture the ice flow dynamics of the LIS from its LGM position to the Younger Dryas ice margin position. The ArcticDEM was the main dataset used for landform mapping (Porter et al., 2018), with the Landsat Image Mosaic of Canada (Government of Canada, 2013) being used as a supplement to identify artefacts or map in blank spots of the ArcticDEM. Much of the area covered has previously been mapped, but the advances in freely-available, high-resolution elevation datasets allow us to map the entire study area with a consistent approach and quality.

Subglacial bedforms (ice flow parallel lineations, $n$=76,630 and subglacial ribs, $n$=2,396) are the most common landforms within the map. Subglacial ribs are typically located in swarms with a similar size and morphology and are located at a range of elevations, from valley floors to high elevation plateaus. They are often superimposed by ice flow parallel lineations. Similarly, ice flow parallel lineations are commonly found in swarms of lineations with a consistent spacing, size and orientation. Cross-cutting relationships are common between different swarms of lineations and record the changing ice flow trajectories over time.

Eskers, moraines, and hummocky terrain are the main record of the ice margin retreat patterns and processes. The map contains a total of 9,833 eskers with a wide range of orientations, although over half of the mapped eskers are located on the Canadian Shield with an east-west orientation due to their deposition at an ice margin retreating to the east. There are 1,022 moraines in the map with a wide range of orientations and morphologies relating to the ice marginal processes and thermal regime. The majority of the hummocky terrain is located in the northwest of the map area, around the Mackenzie Delta and Horton Plain region. While hummocky terrain largely appears chaotic, some areas display a strong linearity and may include sharp-crested ridges.

The map includes 4,308 meltwater channels and 1,338 marginal meltwater channels with a wide range of morphologies. We do not attempt to distinguish between subglacial and proglacial meltwater channels in the 'meltwater channel' category due to the low relief of the investigated region. The low relief of the region means the marginal meltwater channels are relatively rare and where present are restricted to uplands and plateaus where they record the thinning of the ice sheet (e.g. on the Melville Hills).

Other mapped landforms include: perched deltas ($n$=57), raised shorelines ($n$=16,401), and glaciofluvial complexes ($n$=218) that record the extent of glacial lakes that formed during the retreat of the northwestern LIS margin. The map also includes: crevasse fill ridges ($n$=2,110), shear margin moraines ($n$=7), and aeolian dunes ($n$=496). While aeolian dunes are not a glacial feature, they typically are formed from glacial lake sediments immediately following the drainage of these lakes and may be misinterpreted as ice flow parallel lineations, and so are included for completeness.

## 4.3 Paper III

Stoker, B.J., Margold, M., Gosse, J.C., Hidy, A.J., Monteath, A.J., Young, J.M., Gandy, N., Gregoire, L.J., Norris, S.L. and Froese, D., 2022. The collapse of the Cordilleran–Laurentide ice saddle and early opening of the Mackenzie Valley, Northwest Territories, Canada, constrained by $^{10}$Be exposure dating. *The Cryosphere*, *16*(12), pp.4865-4886

In this paper, we use terrestrial cosmogenic nuclide exposure dating with in-situ produced $^{10}$Be from glacial erratics at six sites in the central Mackenzie Valley, Northwest Territories, to provide the first direct constraints on the timing of deglaciation for this region. We combine the exposure ages with the pre-existing radiocarbon constraints in a Bayesian framework to determine the rate of ice sheet thinning, ice margin retreat rates and the retreat pattern of the northwestern LIS. Using this new chronology, we investigate the implications for the regional ice margin timing and pattern, the opening of the Mackenzie Valley and the contribution to past global mean sea level rise.

We use the online exposure age calculator CRONUS-Earth of Balco et al. (2008; version 3.0) and apply a GIA correction. We sampled two sites that are at the LGM limit of the LIS. The samples from Dark Rock Creek were taken from quartzite boulders that matched the local lithology and the exposure ages were poorly clustered, ranging from 24.1±2.0 ka to 254.9±20.3 ka. We attribute the poor clustering to inherited signal due to the short transport history of the boulders that meant there was not significant enough erosion to reset the cosmogenic signal. The remaining presented site deglaciation ages are calculated from our Bayesian model. At our second LGM site, Katherine Creek, our three exposure ages were well-clustered and resulted in a deglacial site age of 15.8 ka (17.1 – 14.6 ka) for a ridgeline west of the Mackenzie Valley at an elevation of ~1,200 m and latitude of ~65°N. East of the Mackenzie River at ~65°N, two samples at the Norman Range site (elevation ~900 m) provide a deglaciation age of 14.2 ka (15.0 – 13.6 ka) and four samples from the adjacent Mackenzie Valley floor (~200 m elevation) provide a deglaciation age of 13.6 ka (14.1 – 13.2 ka), with one sample rejected as an outlier. Together these sites constrain the rate of ice sheet thinning. Two sites were sampled in the Franklin Mountains at ~63°N to further constrain the rate of ice sheet thinning. The first site, near the summit of Cap Mountain (~1450 m elevation) provided a deglaciation age of 14.9 ka (15.6 – 14.2 ka), with two samples rejected as outliers. The second site in the lower Franklin Mountains (~800 m elevation) included no outliers and provided a deglaciation age of 14.3 ka (15.1 – 13.6 ka).

Our new chronological model is in broad agreement with the existing age constraints from the northwestern LIS but conflicts with the existing deglacial isochrones for the northwestern LIS and necessitate a revision of the ice margin retreat pattern. The deglaciation of the Norman Range (~900 m, ~65°N) occurred at ~14.2 ka, roughly coincident with the lower Franklin Mountains deglaciation (~800 m, ~62°N) at ~14.3 ka. The previous ice margin chronology suggested the deglaciation of the Norman Range should have occurred before the lower Franklin Mountains, with the ice margin retreating to the south. Instead, our constraints suggest the ice margin retreat was to the east. Additionally, these constraints indicate that the retreat of this ice sheet sector occurred around 1,000 years earlier than in previous radiocarbon-based reconstructions (Dyke et al., 2003; Dalton et al., 2020; Figure 2).

The large uncertainties associated with terrestrial cosmogenic nuclide exposure dating mean that it is not possible to calculate exact rates of ice sheet thinning. However, ice sheet thinning of ~800 m over our vertical sampling transects occurs within the ~1,000 year resolution of exposure dating, so must have been relatively rapid. These constraints, along with the broad chronological sequence of deglaciation, provide support for the hypothesised ice saddle collapse proposed by Gregoire et al. (2015). As such, we matched these model simulations to our chronology and identified 15 compatible numerical modelling simulations. The contribution to sea level rise of this ice sheet sector was then calculated for each model simulation. Using an average of all 15 model simulations, we found that during deglaciation the ice saddle region likely contributed 13.4 m to global mean sea level rise, with the majority of this sea level rise (11.2 m) occurring between 16 ka and 13 ka.

The advance of the LIS into the Mackenzie Valley blocked the migration of fauna and early humans between Beringia and North America and dammed glacial lakes. The timing of ice-free conditions provides an important constraint on these events. Our exposure ages indicate that ice remained in the Mackenzie Valley until ~13.6 ka (14.1 – 13.2 ka) and obstructed glacial lake drainage and the migration of flora and fauna until after this time.

## 4.4 Paper IV

Stoker, B.J., Dulfer, H.E., Stokes, C.R., Brown, V.H., Clark, C.D., Ó Cofaigh, C., Evans, D.J.A., Froese, D., Norris, S.L. and Margold, M. *in review.* The ice flow dynamics of the northwestern Laurentide Ice Sheet during the last deglaciation. Submitted to *The Cryosphere, Special Issue: Icy landscapes of the past.*

In this paper, we reconstruct the ice flow dynamics and ice margin retreat processes of the northwestern LIS through the last deglaciation using the glacial geomorphological map produced in paper II. We classify distinct swarms of glacial lineations into 326 flowsets based on their morphology and association with other landforms and divide them into four categories that are defined by the ice flow regime and the position of formation within the ice sheet. Ice stream flowsets are composed of highly elongate lineations and are indicative of fast ice flow. Deglacial and inferred deglacial flowsets are interpreted to have formed near to the ice sheet margin due to their association with deglacial landforms or lineation morphology. Event flowsets were formed towards the interior of the ice sheet and are often fragmented and are not associated with deglacial landforms. Cross-cutting relationships are then used to identify the relative sequence of ice flow which is constrained in time with the ice margin chronology of Dalton et al. (2023).

The ice flow drainage network evolved through time in response to changing ice source areas during deglaciation. At the LGM, ice flow was predominantly directed to the north or northwest from the Cordilleran-Laurentide ice saddle in the south or the Keewatin Ice Dome in the east. The ice flow drainage network underwent a rapid reorganisation during the Bølling–Allerød as the northerly ice flow was replaced by westerly ice flow. The change in ice flow orientation is indicative of the relatively rapid loss of the Cordilleran-Laurentide ice saddle compared to the Keewatin Ice Dome.

We reconstruct significant changes in ice stream activity during the deglaciation. Ice stream activity peaked early during the Bølling–Allerød and subsequently declined. We associate the peak in ice stream activity with a climatically-driven steepening of the ice sheet surface profile which increased the driving stresses in the ice sheet interior. High rates of ice streaming were facilitated by a deformable, subglacial soft-bed and high calving rates at lacustrine margins. Rapid ice drawdown during increased ice streaming led to a thinner ice sheet profile and a reduction in ice stream activity. As the margin retreated on to the Canadian Shield at the start of the Younger Dryas, the hard-bed conditions and absence of glacial lakes contributed to the complete cessation of ice streaming in the thin ice sheet.

Dynamic ice margin retreat processes dominated during deglaciation, although the regional geomorphological signatures are complex and display a clear zonation of retreat processes and ice marginal thermal regime. The initial deglaciation was characterised by the pulsed retreat of a polythermal margin with controlled moraines recording the readvances of surging ice lobes. As deglaciation continued, pulsed ice margin retreat continued but the thermal regime became dominated by warm-based conditions. Localised areas of recessional moraines around the Norman Range record the active retreat of a warm-based ice lobe. Widespread ice stagnation is not observed for the northwestern LIS. Instead, evidence of stagnation is generally limited to small, upland plateaus.

# 5.0 Discussion

## 5.1 Cosmogenic nuclide exposure age calculation

Terrestrial cosmogenic nuclide exposure dating includes considerable uncertainties relating to the calculation approach chosen by users. In the previous three years there have been four new exposure age datasets published for the western LIS (Clark et al., 2022; Norris et al., 2022; Reyes et al., 2022; Stoker et al., 2023). These publications follow different approaches for calculating exposure ages, including different production rates, scaling models, and methods of GIA correction. This results in chronological constraints on the western LIS deglaciation that are not internally consistent and site deglaciation ages that conflict with each other and the established ice margin retreat patterns (see Figure 3). To allow comparability between each publication a standardised approach for calculating the exposure ages should be followed. As there are no strict rules on the exposure age calculation approach for each site and region, each study must carefully consider the site characteristics on a case-by-case basis to identify the most appropriate steps for developing a robust chronology.

In paper III, we performed a sensitivity analysis to compare different exposure age calculation approaches on the reconstructed timing of deglaciation. Our sites are located in the mid-latitudes at a range of high and low elevations and are all pre-Holocene. As such, we opted to use the global production rate (Borchers et al., 2015) which covers a range of latitudes (up to 57°N), elevations (130 – 4900 m), and exposure ages (~11 – 18 ka) that make it almost universally applicable. Additionally, since these sites are not solely located in formerly glaciated regions, the production rate has not been influenced by the effects of GIA and allows the user to apply their own GIA correction. Finally, we use the time-dependent LSDn scaling model (Lifton et al., 2014). This is a similar approach to that applied by Norris et al. (2022), with the only difference being that Norris et al. (2022) applied a more sophisticated approach to correct for GIA.

Clark et al. (2022) and Reyes et al. (2022) both followed an exposure age calculation approach that used the Arctic Production rate (Young et al., 2013), the Lal/Stone scaling model (St scaling scheme; Balco et al., 2008), and the same correction approach for GIA used by Norris et al. (2022). We found that this 'alternate' exposure age calculation approach results in exposure ages that are ~10% older than the approach applied in paper III. The scaling model choice is a relatively minor influence on the calculated age, resulting in only ~2% difference, while the production rate has a major influence as ages calculated with the Arctic production rate were ~8.5% older than exposure ages calculated using the global production rate. The GIA correction approach employed by Reyes et al. (2022) and Clark et al. (2022) also resulted in exposure ages that were ~3.5% older than exposure ages calculated following our approach.

The reconstructed timing of deglaciation for each approach was compared to the pre-existing independent constraints on the timing of deglaciation. We found that our approach using the global production rate, LSDn scaling model and a GIA correction approach produced a deglacial chronology that was more compatible with the existing empirical data. The alternate exposure age calculation approach produced ages that were largely too old to be compatible with the existing age constraints. This incompatibility is largely the result of the application of a GIA correction to exposure ages calculated using the Arctic production rate. The sites in the Baffin Bay that comprise the Arctic production rate have been influenced by the effects of GIA. This means that the calculated production rate has an inherent element of GIA included and so it is inappropriate to add a correction for GIA to ages calculated using the Arctic production rate. In fact, Young et al. (2013) provided an alternate production rate for their sites with the influence of GIA removed to address this issue and allow users to apply their own GIA correction. The issue of compounding GIA corrections on exposure age calculation has previously been highlighted (Young et al., 2013; Young et al., 2020) and results in exposure ages that are likely too old. The application of a uniform approach to calculating exposure ages also creates an internally consistent dataset and removes any conflicting deglaciation ages. This highlights the large uncertainties involved in cosmogenic nuclide exposure dating and the importance of communicating these uncertainties and justifying the choices made so that it is comprehensible to non-experts.

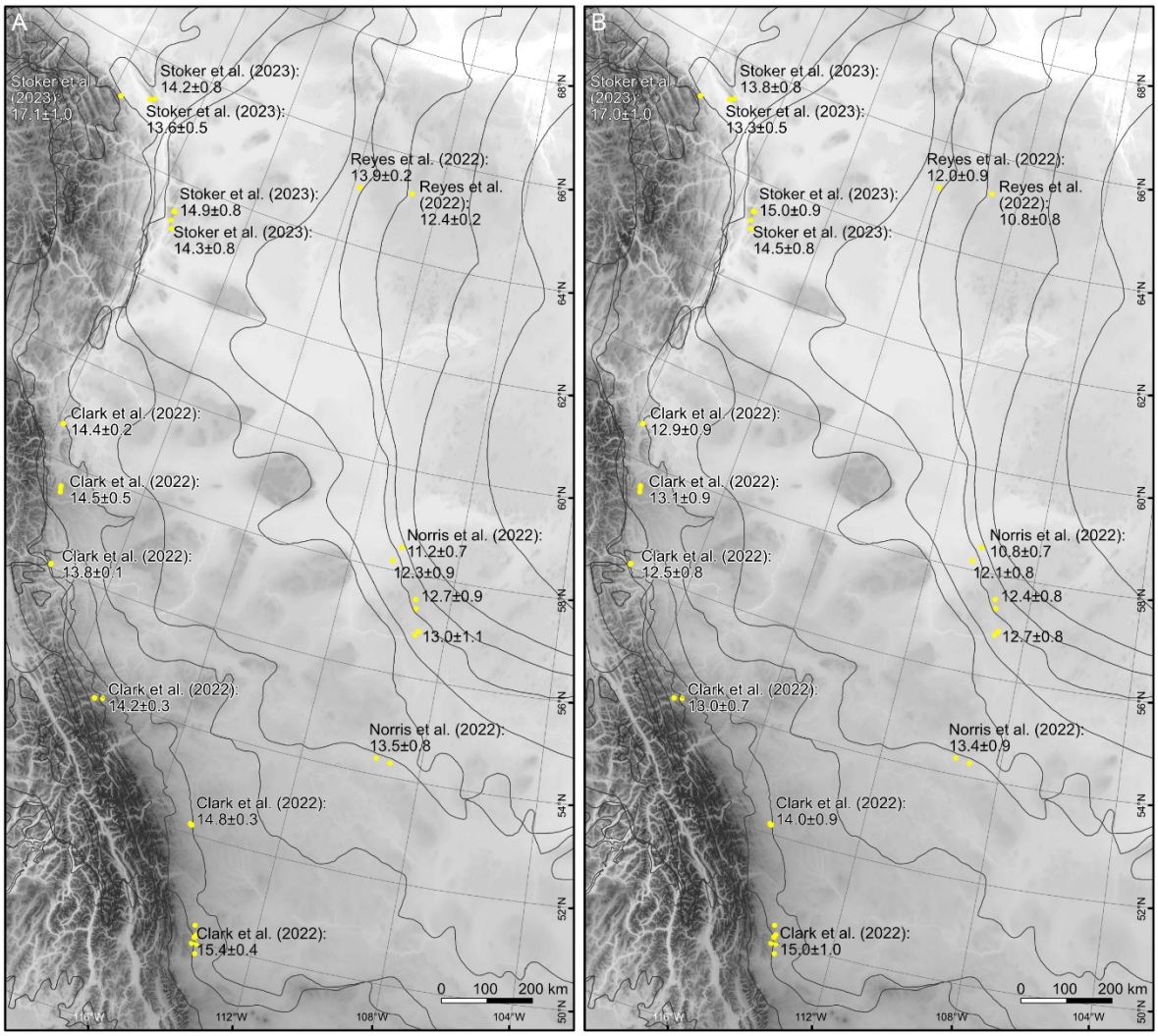


Figure 3: A comparison of how the published cosmogenic nuclide exposure ages for the western LIS compare to exposure ages calculated using a different, uniform approach. The ice margin retreat pattern of Dyke et al. (2003) is used to indicate the expected retreat pattern of the western LIS. The timing of ice margin location is left intentionally absent as these ice margins are based on an outdated radiocarbon chronology. However, the margin retreat pattern is principally based on geomorphology. The more recent ice margin retreat pattern of Dalton et al. (2023) is based on the cosmogenic nuclide exposure age chronology in some locations. As such, using the retreat pattern of Dalton et al. (2023) would effectively mean comparing the exposure ages against a retreat pattern based on exposure ages. While the Dyke et al. (2003) retreat pattern provides an independent, geomorphology-based retreat pattern for comparison. Note the conflicting deglaciation ages between sites that is largely resolved by calculating exposure ages with a standardised approach. (A) The site deglaciation ages across the western LIS as presented by the original authors. (B) The site deglaciation ages calculated using the ExPage calculator (Heyman, 2024). Sites are presented as a simple mean age with outliers described by the original authors excluded.

## 5.2 The response of the northwestern Laurentide Ice Sheet to changes in climate during the last deglaciation

Prior to this thesis, the response of the northwestern LIS to climate oscillations during the last glacial termination was poorly constrained. Previous radiocarbon-based chronologies suggested slow retreat during the Bølling–Allerød warm period followed by rapid retreat during the Younger Dryas (Dyke et al., 2003; Dalton et al., 2020; Figure 2A). However, numerical modelling studies have suggested that the northwestern LIS responded to warming during the Bølling–Allerød by undergoing rapid ice sheet thinning in the Cordilleran-Laurentide ice saddle region (Gregoire et al., 2016). In paper III, we identify a period of rapid ice sheet thinning during the Bølling–Allerød using cosmogenic nuclide exposure

dating along vertical elevation transects that provides support for these numerical modelling simulations. Additionally, other studies have confirmed a reduction in the ice margin retreat rates on the Canadian Shield during the Younger Dryas (Reyes et al., 2022; Figure 2B). However, the response of the ice sheet to these climatic events is unknown in regard to the evolution of the ice drainage network, the drivers of ice streaming, and the dominant ice margin retreat processes. In paper IV, we reconstruct the dynamics of the northwestern LIS during deglaciation. However, many uncertainties remain in this reconstruction that are discussed below.

## 5.3 Ice drainage network evolution

The previous reconstruction of the ice flow dynamics of the northwestern LIS was limited by the low-resolution of the remote sensing data available at the time (Brown, 2012). In paper IV, we take advantage of newly-available high-resolution data to provide the first detailed reconstruction of the evolution of the ice flow network during the last deglaciation. The Keewatin Ice Dome, located in the east, and the Cordilleran-Laurentide ice saddle, located in the south, were the two ice source areas that fed the ice drainage network of the northwestern LIS (Figure 1B). During the LGM, ice flow was predominantly directed to the north or north-west, indicating a significant contribution to ice flow by the ice saddle region. During the Bølling–Allerød, the ice drainage network underwent a rapid reorganisation to westerly ice flow from the Keewatin Ice Dome. The change in ice flow direction supports the hypothesis of rapid ice sheet thinning in the ice saddle region as the Keewatin Ice Dome remained stable enough to maintain westerly ice flow into the Mackenzie Mountains range front while the ice saddle had completely disappeared.

## 5.4 Ice stream switching

Margold et al. (2018) highlighted that the Mackenzie Trough Ice Stream represented a key uncertainty in our understanding of the ice stream network of the northwestern LIS. Whether the Mackenzie Trough Ice Stream was an extensive ice stream system that migrated laterally into the Anderson Plain during deglaciation or operated as a series of small, time-transgressive ice streams near the ice sheet margin was an unresolved issue.

In paper IV, the morphology of glacial lineations records the alternating activity of the Mackenzie Trough and Anderson ice streams. Highly-elongate glacial lineations in the offshore record indicate that the Mackenzie Trough Ice Stream was active during the LGM (Batchelor et al., 2013). Following ice margin retreat to around 68°N, lineations are less elongate and indicative of a slower ice flow regime in the Mackenzie Delta region, while highly elongate lineations over the Anderson Plain record Anderson Ice Stream switch-on. By the time the ice margin had retreated to ~67°N in the Mackenzie Valley, highly elongate glacial lineations record the return to a fast ice flow regime indicative of ice streaming as the large Bear Lake Ice Stream flowed into both the Mackenzie Valley and the Anderson Plain.

The evolution of the ice streaming network is relatively well-constrained, but the reasons for ice stream migration are less clear. One possible explanation could relate to the proximity of the Amundsen Gulf Ice Stream and the buttressing force it provides. During the build-up to the LGM, the Amundsen Gulf Ice Stream advanced across the northern side of the Anderson Plain and buttressed ice flow through the region. The more distal position of the Mackenzie Trough from the Amundsen Gulf Ice Stream may have allowed the establishment of the Mackenzie Trough Ice Stream. During deglaciation, the retreat of the Amundsen Gulf Ice Stream removed the buttressing force from the Anderson Plain ice and may have triggered the Anderson Ice Stream. Alternatively, as the Mackenzie Trough Ice Stream retreated back onshore during the early deglaciation, ice flow may have reduced due to reduced calving at the terrestrial margin and caused the stagnation of an ice lobe in the Mackenzie Delta region. This stagnant ice may have obstructed ice flow through the Mackenzie Trough Ice Stream and forced ice drainage through the newly established Anderson Ice Stream.

## 5.5 Ice streaming and ice sheet mass balance

The delivery of ice from the ice sheet interior to the ice sheet margin through fast-flowing ice streams can contribute to a negative ice sheet mass balance by increasing calving at the margin and through the drawdown of ice to lower elevations where it experiences higher rates of surface melting (Robel and Tziperman, 2016). The ice stream network of the northwestern LIS is one of the most poorly understood (Margold et al., 2018). In paper IV, we reconstruct how ice stream activity varied through time to investigate the drivers of ice stream activity and the implications for ice sheet mass balance.

The changing ice stream activity can be largely explained by climate-driven variations in the ice sheet surface slope. Warming during the Bølling–Allerød caused an expansion of the ablation area as the ELA lowered (Figure 4). This resulted in a steepening of the ice sheet surface slope and increased driving stresses in the ice sheet interior which led to the peak in ice stream activity. Enhanced ice streaming was facilitated by reduced basal drag due to the soft subglacial bed and high calving rates at widespread lacustrine margins across the Northern Interior Plains. High rates of ice streaming led to the rapid drawdown of ice from the ice sheet interior to the margin and contributed to a negative mass balance. Ice drawdown thinned the ice sheet profile and caused a reduction in ice stream activity.

All ice stream activity stopped by the start of the Younger Dryas, as the thin ice sheet profile was further stabilised by the retreat of the ice sheet margin on to the hard-bed of the Canadian Shield which increased frictional drag (Figure 4). Calving rates were also reduced as the ice sheet margin became terrestrially terminating. The reduced ice stream activity combined with cooling during the Younger Dryas should have caused a more positive ice sheet mass balance and led to the stabilisation of the ice sheet margin. However, ice margin retreat continued during the Younger Dryas, albeit at a slower rate than during the Bølling–Allerød.

While our reconstruction does not extend far enough to provide a detailed reconstruction of the ice dynamics changes during the Younger Dryas and into the Holocene, it is interesting to speculate about how the rapid ice sheet thinning and ice drawdown during the Bølling–Allerød may have influenced the later ice sheet retreat. For example, the thin ice sheet profile created by rapid ice drawdown may have been inherently unstable and vulnerable to continued retreat despite Younger Dryas cooling. This continued retreat of the ice sheet margin between 110°W and ~103°W would have slowly steepened the ice sheet surface slope and increased driving stresses. The fact that ice streaming did not resume until the ice sheet margin retreated to ~103°W might suggest that the ice sheet profile remained too thin to generate the high driving stresses required for ice streaming, with the frictional drag of the hard-bed providing a further stabilising influence on ice flow. The development of the Dubawnt Lake may have provided a trigger to initiate the Dubawnt Lake Ice Stream after the ice sheet profile had steepened enough (Stokes and Clark, 2003). It is also possible that the positive mass balance effect of reduced ablation due to Younger Dryas cooling may have been offset if accumulation was also reduced due to lower precipitation values, contributing to the continued ice margin retreat. However, a poor understanding of the palaeoclimatic changes in the region since the LGM mean that this is difficult to prove.

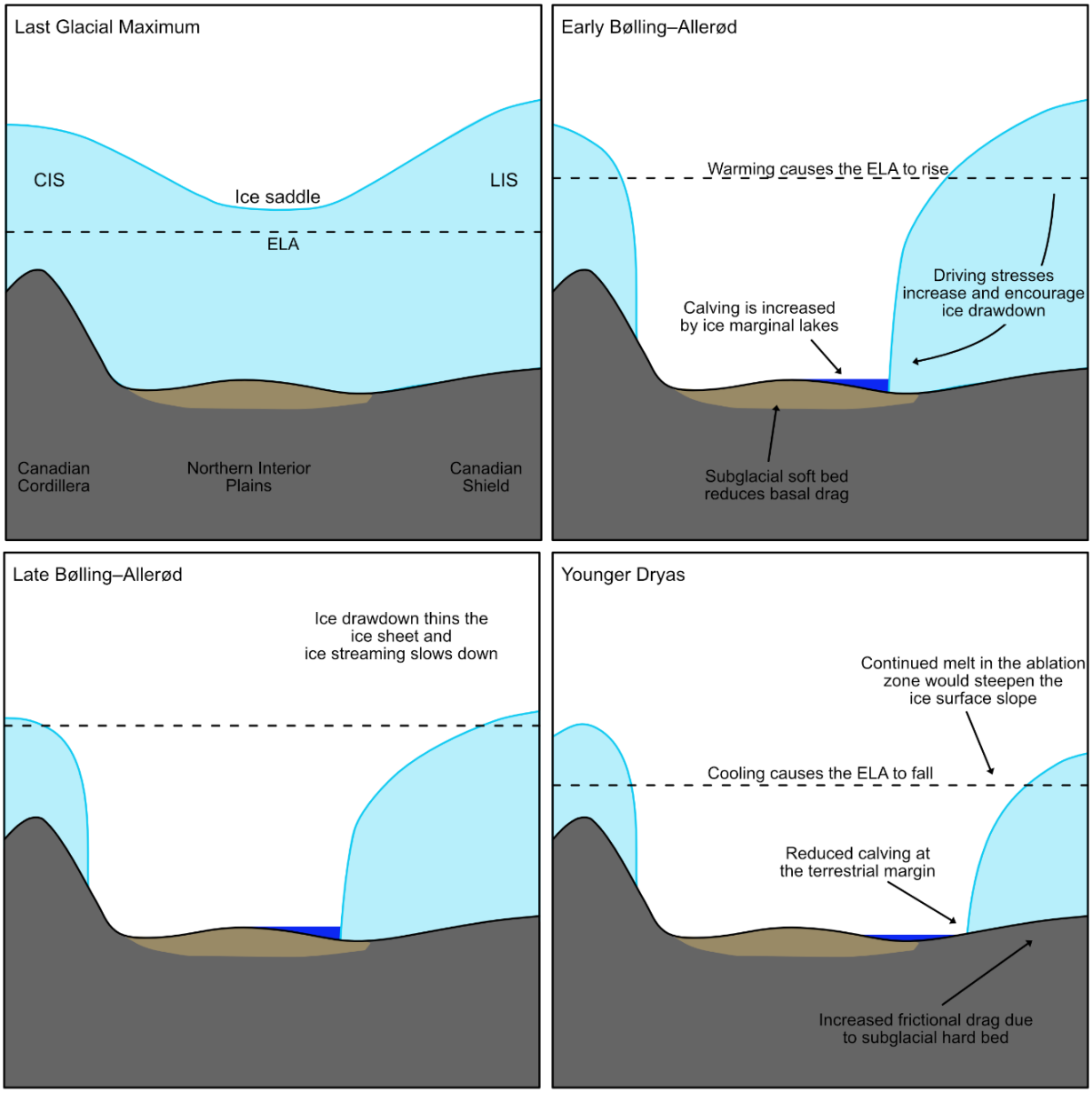


Figure 4: A schematic illustration of how changing climate can influence the ice sheet surface slope and ice stream activity. Note, ice sheet separation is depicted as occurring in the 'Early Bølling-Allerød' based on the timing of separation in Dalton et al. (2023) and retreat onto the Canadian Shield at the start of the Younger Dryas is also based on this temporal framework.

## 5.6 The ice margin retreat processes

Dyke and Evans (2014) identified a clear zonation in the ice margin retreat processes during the retreat of the northwestern LIS. In paper IV, we reconstruct the ice margin retreat processes and find a similar zonation that is largely similar to the classification of Dyke and Evans (2014). In the north, the initial retreat of the northwestern LIS was dominated by the pulsed retreat of a debris-rich, polythermal margin. There is limited evidence of ice margin stagnation, and the identified areas of stagnation are often limited in spatial extent. During deglaciation, ice margin retreat processes remained dynamic, but the thermal regime became more warm-based with local areas of active ice margin recession. During this time, stagnation was localised to the uplands between ice streams. The retreat of the ice margin across the Canadian Shield to 110°W was also dominated by dynamic ice margin retreat as recorded by ice-marginal indicators (e.g. flat-topped eskers) and the changing ice flow patterns. In our reconstruction, the northwestern LIS responded to the rapid change in the ice sheet geometry during Bølling-Allerød by continued, dynamic ice margin retreat.

The southwestern LIS underwent a similar period of rapid retreat during the Bølling-Allerød. Despite being fed by the same two ice sources, the Keewatin Ice Dome and the Cordilleran-Laurentide ice saddle, the southwestern LIS margin responded to this change in ice sheet geometry by relatively extensive ice sheet stagnation punctuated by surging ice lobes (Norris et al., 2023). The exact causes for the different ice margin retreat processes are unclear. Here we suggest two possible, speculative explanations:

- The relatively warmer climate of the southwestern LIS means that the ELA is relatively higher than for the northwestern LIS. Larger areas of the southwestern margin were likely located below the ELA, which could have contributed to more widespread surface melting and ice sheet thinning. The relatively colder temperatures of the northwestern margin likely meant that larger areas of the northwestern sector were located above the ELA and surface melting was less common.
- The southwestern ice sheet margin was more dependent on the Cordilleran-Laurentide ice saddle as an ice source area as it was located in a more distal location from the Keewatin Ice Dome. The rapid loss of the ice saddle as a source region may have left large areas of the southwestern margin 'stranded' and vulnerable to in-situ stagnation. Margold et al. (2018) reconstruct a northerly migration of the Keewatin Ice Dome during deglaciation that places it in a more proximal location to the northwestern margin and might have allowed the Keewatin Ice Dome to continue to sustain dynamic ice margin retreat while the southwestern margin was left isolated and vulnerable to stagnation.

# 6.0 Future work

## 6.1 The pre-LGM history of the Laurentide Ice Sheet

The inaccessible nature of much of northwestern Canada means that our understanding of the configuration and extent of glaciations prior to the LGM is poor and there are many contradictions in the existing reconstructions. Initially, the glacial stratigraphy in northwestern Canada was interpreted as representing multiple cycles of localised montane or plateau ice caps prior to the LGM (Duk-Rodkin and Barendregt, 2011). A recent re-interpretation of the stratigraphy in the Horton Plain identified at least one advance of the LIS at ~2.9 ma and re-interpreted multiple till sequence as a complex sequence of thrust stacking during glacitectonism from the LIS (Evans et al., 2021). This evidence of an extensive Keewatin Ice Dome in northwestern Canada is roughly coincident with the first appearance of Labrador sourced ice at 39°N in USA and suggests an early extensive LIS.

The maximum extent of this early ice sheet is unknown and the sparse evidence of pre-LGM glaciations is poorly constrained in time. In the Mackenzie Delta region, borehole core records also indicate an early Matuyama glaciation and no other glaciation until the LGM (Barendregt and Duk-Rodkin, 2004). This early glaciation was originally assumed to relate to a local ice mass (Barendregt and Duk-Rodkin, 2004). But, with the new evidence of an early LIS advance over the adjacent Horton Plain, it is possible to envisage how the LIS might have also extended into the Mackenzie Delta. The offshore record similarly indicates only two glacial advances through the Mackenzie Trough (Batchelor et al., 2013). The initial advance that carved the Mackenzie Trough is suggested to have occurred in the Illinoian or Early Wisconsinan glaciations but is not constrained by any dating methods (Batchelor et al., 2013). It is unclear which age is correct, or whether these two deposits represent two separate, distinct glaciations. In the Amundsen Gulf, there is a long history of multiple ice sheet advances that are suggested to have occurred throughout the Quaternary period (Batchelor et al., 2014). Despite building evidence for pre-LGM LIS glaciations in northwestern Canada, there is currently no evidence that the LIS extended west of the modern-day Mackenzie River prior to the LGM.

There is a clear need to improve our understanding of the timing, extent and number of glaciations that occurred in northwestern Canada throughout the Quaternary. Here we briefly outline some possible avenues of research:

- The reinterpretation of the stratigraphy in the Horton Plain highlights the possibility of revisiting previously documented stratigraphic sections and applying modern advances in glacial sedimentological knowledge to better understand the origin of these sediments. Across the range front of the Mackenzie Mountains there are multiple, well documented sediment sections that may possibly record evidence of an early Laurentide advance to the west of the Mackenzie River.
- The development of cosmogenic nuclide burial dating (e.g. Balco and Rovey, 2010) provides an opportunity to directly date these early glacial advances. This would allow us to not only reconstruct the past extent of these glaciations but also to provide a numerical age for some of these sediments.
- The use of paired cosmogenic nuclides can also provide a greater insight into the glacial history than a single cosmogenic nuclide (e.g. Young et al., 2021). While this approach has been previously applied to bedrock, we identify significant inheritance in some of our newly dated glacial erratics from west of the Mackenzie River (unpublished). The use of a paired isotope approach might allow us to understand the long-term history of these boulders and provide evidence for a pre-LGM glaciation.

## 6.2 The interaction between the ice masses of the Mackenzie Mountains

In paper I, the glacial geomorphological map documents the extent, retreat patterns and relationships between montane ice masses and the Laurentide and Cordilleran ice sheets in the Mackenzie Mountains. However, paper I does not attempt to leverage this map to reconstruct the glacial history of the region.

Across the eastern side of the Mackenzie Mountains, a series of moraines from local montane ice masses are cross-cut by meltwater channels from the LIS (Figure 5A). Shield erratics up to 1 km beyond the LIS meltwater channels were used to suggest an early LIS advance to it's all-time maximum at ~30 ka (Duk-Rodkin and Hughes, 1991; Figure 5C). The retreat of the LIS allowed the growth of montane ice masses and the formation of the montane moraines. The LIS readvanced at ~22 ka and reached a maximum extent marked by the meltwater channels (Figure 5C). However, the hypothesis of a significant readvance is fitted to an outdated chronological model which has since been disproven (Kennedy et al., 2010; paper III). An alternative, simpler model involves the montane ice masses responding rapidly to climate and reaching an early local LGM due to their small size. The large size of the LIS meant that its advance to the maximum was slow and so it only reached its maximum late. As it reached the maximum, the LIS margin was cold-based and non-erosive, so it did not destroy the montane moraines and deposited Shield clasts near the maximum limit. During retreat, the meltwater channels were cut into the montane moraines.

The early advance of montane ice masses to their LGM extent is also supported by cross-cutting relationships in the northern Mackenzie Mountains. A series of montane moraines record the early advance of these montane ice masses to their local LGM position (Figure 5B). Meltwater channels cut into these moraines indicate how a cold-based lobe of the Cordilleran Ice Sheet must have subsequently advanced over these areas, as it reached a later maximum extent.

A similar landform association is observed in the southern Mackenzie Mountains, indicating the rapid response of montane ice masses to climatic oscillations while ice sheets experienced a delayed response time. Montane moraines dated to ~14 ka (Menounos et al., 2017) may indicate a readvance roughly correlated with the Older Dryas climatic cooling event and the meltwater channels incised into these moraines record the later advance of the Cordilleran Ice Sheet (Figure 5D). This readvance may have occurred late during the Older Dryas or even later during the Younger Dryas. This is consistent with the sequence observed in the central Cordilleran Ice Sheet and documented by Dulfer et al. (2022). The extension of this interpretation would allow us to further refine the ice margin chronology and better understand the ice sheet response to the millennial-scale climate events.

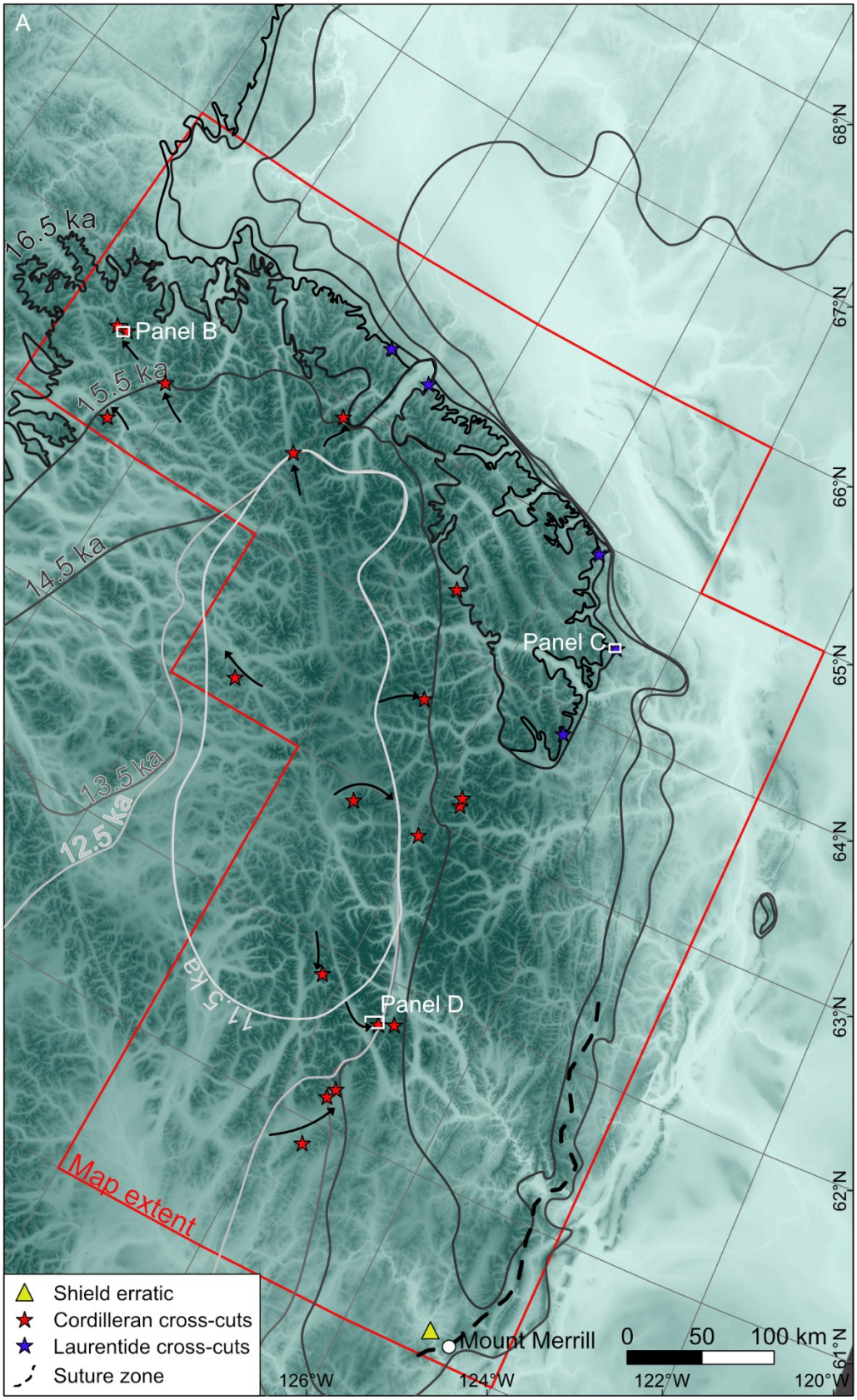


Figure 5: The landform associations in the Mackenzie Mountains. Note how montane landforms are always cross-cut by the landforms from either the Laurentide or Cordilleran ice sheets and the reverse association is not observed. This indicates the relatively rapid response time of the local montane glaciers to climate compared to the ice sheets which lagged behind. (A) The distribution of cross-cutting landform relationships.

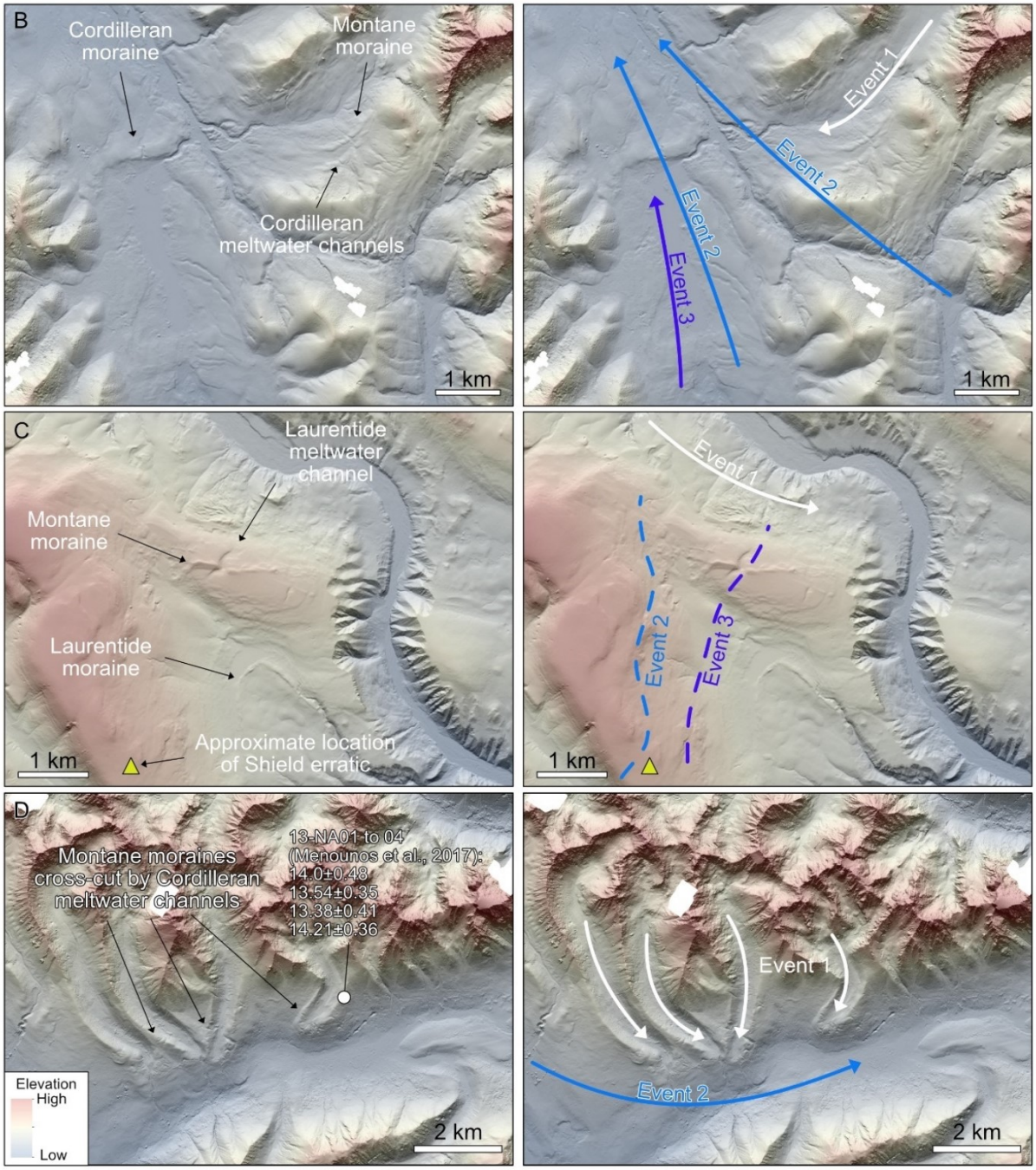


Figure 5: (B) Moraines from a montane ice mass near the LGM limit of the Cordilleran Ice Sheet. Note the meltwater channels cut into the moraines. Event 1 – The early advance of montane ice masses to their maximum extent, forming moraines. Event 2 – The late advance of the Cordilleran Ice Sheet to its maximum extent, overriding montane ice masses and cutting meltwater channels into the moraines. Event 3 – A localised readvance or standstill of the Cordilleran Ice Sheet during retreat forming a moraine. (C) Montane moraines near the Little Bear River cross-cut by meltwater channels from the LIS near it's LGM limit. Event 1 – The early advance of montane glaciers to their maximum extent and moraine formation. Event 2 – The late advance of the cold-based LIS to its maximum extent, overriding the montane glacier and depositing Shield erratics. Event 3 – The retreat position of the LIS, cutting meltwater channels into the montane glacier moraine. (D) Montane moraines that have been dated to before the Younger Dryas period cross-cut by meltwater channels during a readvance of the Cordilleran Ice Sheet. Event 1 – The re-advance of montane glaciers during the Older Dryas. Event 2 – The late response of the Cordilleran Ice Sheet to the Older Dryas or Younger Dryas cooling and readvance over the montane glaciers, cutting meltwater channels into the moraines.

While there are no clear cross-cutting relationships between landforms from the Cordilleran Ice Sheet and LIS, surficial geological maps combined with paper I can be used to identify the relative advance and retreat dynamics of these ice sheets. Smith (2002) identify Shield erratics atop Mount Merrill (~1,400 m) and along the valley floors ~80 km west of Mount Merrill. These erratics record the early advance of the LIS into the southern Mackenzie Mountains that entirely subsumed the topography. Subsequently, the Cordilleran Ice Sheet advanced into the region and must have merged with the LIS. However, no deglacial landforms are identified to the west of Mount Merrill (Figure 5A). This suggests that while the LIS advanced into the region first it also retreated first. Deglacial landforms from the Cordilleran Ice Sheet indicate that it was pressed against the western side of Mount Merrill during deglaciation, further than it had advanced prior to the deglaciation phase. Meltwater channels from both ice sheets well document the suture zone of the ice sheets in this region (Figure 5A, dashed line).

## 6.3 Meltwater drainage and glacial lake history of the northwestern Laurentide Ice Sheet

In this thesis, we reconstruct a period of rapid thinning of the ice saddle region triggered by warming during the Bølling–Allerød (paper III). The collapse of the ice saddle resulted in a rapid reorganisation of the ice drainage network (Paper IV). During this period, the melting of the ice sheet must have produced considerable amounts of meltwater. In paper I, we map a series of large, lateral meltwater spillways that likely record the drainage of meltwater from the northwestern LIS during the Bølling–Allerød (Figure 6). Attempts to understand meltwater drainage through these lateral meltwater spillways are limited to the Southern Mackenzie Mountains (59-60°N; Huntley et al., 2017). However, these channels extend along the range front of the mountains up to 65°N and record the evolution of the meltwater drainage network throughout deglaciation. Future research could use hydraulic modelling to understand how meltwater drainage discharge varied through deglaciation and could reconstruct in detail the drainage pathways of meltwater from the ice sheet and glacial lakes.

Figure 6: A photograph of a lateral meltwater spillway in the eastern Mackenzie Mountains. The channel is ~300 m deep and ~1 km wide.

# 7.0 Conclusions

In this thesis, I have produced a new, high-resolution reconstruction of the northwestern LIS, with a focus on the last deglaciation. The reconstruction has been compared to numerical ice sheet model simulations to understand the response of the northwestern LIS to millennial-scale climate oscillations during the last glacial termination. The glacial geomorphology of much of the Northwest Territories has been mapped (paper I and II). New cosmogenic nuclide exposure ages were used to constrain the rate of ice sheet retreat and thinning (paper II). While the previous ice margin chronology suggested that ice margin retreat was slow during the Bølling–Allerød, our new constraints allowed us to identify a period of rapid ice sheet thinning that was likely triggered by warming during the Bølling–Allerød. Our updated ice margin chronology was used to validate numerical ice sheet modelling simulations and quantify the GMSL rise contribution of the region during deglaciation (paper II). The glacial landform record was then leveraged to investigate how the ice flow dynamics responded to the Bølling–Allerød and Younger Dryas climate events (paper IV). The ice drainage network underwent a rapid reorganisation from predominantly northerly oriented ice flow to westerly oriented ice flow over less than 2,000 years and this supports the idea of relatively rapid thinning in the ice saddle region while the Keewatin Ice Dome remained relatively stable. Ice streaming increased in response to the steepening of the ice sheet surface profile during ice sheet thinning triggered by the Bølling–Allerød warming. This highlights the importance of climate-driven changes in the ice sheet surface slope in controlling ice stream activity. Rapid ice drawdown led to a thin ice sheet profile and the cessation of ice streaming activity. The subglacial bed conditions and presence of glacial lakes played a role in facilitating these ice streaming changes, but further work is needed to determine the relative importance of each factor. Dynamic ice margin retreat processes dominated throughout deglaciation, in contrast with the southwestern margin where the loss of the ice saddle is associated with relatively widespread punctuated stagnation. However, the exact cause of this difference is unclear and should be the subject of future research. This research has managed to resolve some of the uncertainties in previous reconstructions but has also highlighted many avenues for future research. For example, the interactions between different ice masses in the Mackenzie Mountains, the meltwater drainage network during the Bølling–Allerød, and the configuration of pre-LGM glaciations all remain poorly understood.

# 8.0 References


Alley, R.B., 2000. The Younger Dryas cold interval as viewed from central Greenland. *Quaternary Science Reviews*, *19*(1-5), pp.213-226

Applegate, P.J., Urban, N.M., Laabs, B.J., Keller, K. and Alley, R.B., 2010. Modeling the statistical distributions of cosmogenic exposure dates from moraines. *Geoscientific Model Development*, *3*(1), pp.293-307

Bailey, W.G., Oke, T.R. and Rouse, W.R., 1997. *Surface climates of Canada* (Vol. 4). McGill-Queen's Press-MQUP

Balco, G. and Rovey, C.W., 2010. Absolute chronology for major Pleistocene advances of the Laurentide Ice Sheet. *Geology*, *38*(9), pp.795-798

Balco, G., 2011. Contributions and unrealized potential contributions of cosmogenic-nuclide exposure dating to glacier chronology, 1990–2010. *Quaternary Science Reviews*, *30*(1-2), pp.3-27

Balco, G., Briner, J., Finkel, R.C., Rayburn, J.A., Ridge, J.C. and Schaefer, J.M., 2009. Regional beryllium-10 production rate calibration for late-glacial northeastern North America. *Quaternary Geochronology*, *4*(2), pp.93-107

Balco, G., Stone, J.O., Lifton, N.A. and Dunai, T.J., 2008. A complete and easily accessible means of calculating surface exposure ages or erosion rates from 10Be and 26Al measurements. *Quaternary Geochronology*, *3*(3), pp.174-195

Barendregt, R.W. and Duk-Rodkin, A., 2011. Chronology and extent of Late Cenozoic ice sheets in North America: a magnetostratigraphical assessment. In *Developments in Quaternary Sciences* (Vol. 15, pp. 419-426). Elsevier

Barth, A.M., Marcott, S.A., Licciardi, J.M. and Shakun, J.D., 2019. Deglacial thinning of the Laurentide Ice Sheet in the Adirondack Mountains, New York, USA, revealed by 36Cl exposure dating. *Paleoceanography and Paleoclimatology*, *34*(6), pp.946-953

Batchelor, C.L., Dowdeswell, J.A. and Pietras, J.T., 2013. Seismic stratigraphy, sedimentary architecture and palaeo-glaciology of the Mackenzie Trough: evidence for two Quaternary ice advances and limited fan development on the western Canadian Beaufort Sea margin. *Quaternary Science Reviews*, *65*, pp.73-87

Batchelor, C.L., Dowdeswell, J.A. and Pietras, J.T., 2014. Evidence for multiple Quaternary ice advances and fan development from the Amundsen Gulf cross-shelf trough and slope, Canadian Beaufort Sea margin. *Marine and Petroleum Geology*, *52*, pp.125-143

Batchelor, C.L., Margold, M., Krapp, M., Murton, D.K., Dalton, A.S., Gibbard, P.L., Stokes, C.R., Murton, J.B. and Manica, A., 2019. The configuration of Northern Hemisphere ice sheets through the Quaternary. *Nature communications*, *10*(1), p.3713

Bednarski, J.M., 2008. Landform assemblages produced by the Laurentide Ice Sheet in northeastern British Columbia and adjacent Northwest Territories—constraints on glacial lakes and patterns of ice retreat. *Canadian Journal of Earth Sciences*, *45*(5), pp.593-610

Borchers, B., Marrero, S., Balco, G., Caffee, M., Goehring, B., Lifton, N., Nishiizumi, K., Phillips, F., Schaefer, J. and Stone, J., 2016. Geological calibration of spallation production rates in the CRONUS-Earth project. *Quaternary Geochronology*, *31*, pp.188-198

Broecker, W., Bond, G. and McManus, J., 1993. Heinrich events: Triggers of ocean circulation change? In *Ice in the Climate System* (pp. 161-166). Springer Berlin Heidelberg

Broecker, W.S., 1998. Paleocean circulation during the last deglaciation: a bipolar seesaw? *Paleoceanography*, *13*(2), pp.119-121

Broecker, W.S., Kennett, J.P., Flower, B.P., Teller, J.T., Trumbore, S., Bonani, G. and Wolfli, W., 1989. Routing of meltwater from the Laurentide Ice Sheet during the Younger Dryas cold episode. *Nature*, *341*(6240), pp.318-321

Brown, V., 2012. *Ice stream dynamics and pro-glacial lake evolution along the north-western margin of the Laurentide Ice Sheet* (Doctoral dissertation, Durham University)

Buizert, C., Gkinis, V., Severinghaus, J.P., He, F., Lecavalier, B.S., Kindler, P., Leuenberger, M., Carlson, A.E., Vinther, B., Masson-Delmotte, V. and White, J.W., 2014. Greenland temperature response to climate forcing during the last deglaciation. *Science*, *345*(6201), pp.1177-1180

Burn, C.R., 1994. Permafrost, tectonics, and past and future regional climate change, Yukon and adjacent Northwest Territories. *Canadian Journal of Earth Sciences*, *31*(1), pp.182-191

Catto, N.R., 1986. Quaternary Sedimentology and Stratigraphy, Peel Plateau and Richardson Mountains, Yukon and Northwest Territories. Unpublished Ph.D. thesis, University of Alberta, Edmonton, Alberta.

Chandler, B.M., Lovell, H., Boston, C.M., Lukas, S., Barr, I.D., Benediktsson, Í.Ö., Benn, D.I., Clark, C.D., Darvill, C.M., Evans, D.J., Ewertowski, M.W., Loibl, D., Margold, M., Otto, J.-C., Roberts, D.H., Stokes, C.R., Storrar, R.D., and Stroeven A.P., 2018. Glacial geomorphological mapping: A review of approaches and frameworks for best practice. *Earth Science Reviews*, *185*(November 2017), pp.806–846. https://doi.org/10.1016/j.earscirev.2018.07.015

Clark, C.D., 1997. Reconstructing the evolutionary dynamics of former ice sheets using multi-temporal evidence, remote sensing and GIS. *Quaternary Science Reviews*, *16*(9), pp.1067-1092

Clark, C.D., Ely, J.C., Greenwood, S.L., Hughes, A.L., Meehan, R., Barr, I.D., Bateman, M.D., Bradwell, T., Doole, J., Evans, D.J. and Jordan, C.J., 2018. BRITICE Glacial Map, version 2: a map and GIS database of glacial landforms of the last British–Irish Ice Sheet. *Boreas*, *47*(1), pp.11-e8.

Clark, J., Carlson, A.E., Reyes, A.V., Carlson, E.C., Guillaume, L., Milne, G.A., Tarasov, L., Caffee, M., Wilcken, K. and Rood, D.H., 2022. The age of the opening of the Ice-Free Corridor and implications for the peopling of the Americas. *Proceedings of the National Academy of Sciences*, *119*(14), p.e2118558119

Clark, P.U. and Mix, A.C., 2002. Ice sheets and sea level of the Last Glacial Maximum. *Quaternary Science Reviews*, *21*(1-3), pp.1-7

Clark, P.U. and Pollard, D., 1998. Origin of the middle Pleistocene transition by ice sheet erosion of regolith. *Paleoceanography*, *13*(1), pp.1-9

Clark, P.U., Pisias, N.G., Stocker, T.F. and Weaver, A.J., 2002. The role of the thermohaline circulation in abrupt climate change. *Nature*, *415*(6874), pp.863-869

Curry, B.B., Lowell, T.V., Wang, H. and Anderson, A.C., 2018. Revised time-distance diagram for the Lake Michigan Lobe, Michigan subepisode, Wisconsin episode, Illinois, USA. In A.E. Kehew, B.B. Curry (Eds.), Quaternary Glaciation of the Great Lakes Region: Process, Landforms, Sediments, and Chronology, Geological Society of America Special Paper 530, pp. 69-101.

Cuzzone, J.K., Clark, P.U., Carlson, A.E., Ullman, D.J., Rinterknecht, V.R., Milne, G.A., Lunkka, J.P., Wohlfarth, B., Marcott, S.A. and Caffee, M., 2016. Final deglaciation of the Scandinavian Ice Sheet and implications for the Holocene global sea-level budget. *Earth and Planetary Science Letters*, 448, pp.34-41

Dalton, A.S., Dulfer, H.E., Margold, M., Heyman, J., Clague, J.J., Froese, D.G., Gauthier, M.S., Hughes, A.L., Jennings, C.E., Norris, S.L. and Stoker, B.J., 2023. Deglaciation of the north

American ice sheet complex in calendar years based on a comprehensive database of chronological data: NADI-1. *Quaternary Science Reviews*, *321*, p.108345

Dalton, A.S., Dulfer, H.E., Margold, M., Heyman, J., Clague, J.J., Froese, D.G., Gauthier, M.S., Hughes, A.L., Jennings, C.E., Norris, S.L. and Stoker, B.J., 2023. Deglaciation of the north American ice sheet complex in calendar years based on a comprehensive database of chronological data: NADI-1. *Quaternary Science Reviews*, *321*, p.108345

Dalton, A.S., Finkelstein, S.A., Barnett, P.J. and Forman, S.L., 2016. Constraining the late Pleistocene history of the Laurentide ice sheet by dating the Missinaibi Formation, Hudson Bay Lowlands, Canada. *Quaternary Science Reviews*, *146*, pp.288-299

Dalton, A.S., Finkelstein, S.A., Forman, S.L., Barnett, P.J., Pico, T. and Mitrovica, J.X., 2019. Was the Laurentide Ice Sheet significantly reduced during marine isotope stage 3? *Geology*, *47*(2), pp.111-114

Dalton, A.S., Margold, M., Stokes, C.R., Tarasov, L., Dyke, A.S., Adams, R.S., Allard, S., Arends, H.E., Atkinson, N., Attig, J.W. and Barnett, P.J., 2020. An updated radiocarbon-based ice margin chronology for the last deglaciation of the North American Ice Sheet Complex. *Quaternary Science Reviews*, *234*, p.106223

Dalton, A.S., Stokes, C.R. and Batchelor, C.L., 2022. Evolution of the Laurentide and Innuitian ice sheets prior to the Last Glacial Maximum (115 ka to 25 ka). *Earth-Science Reviews*, *224*, p.103875

De Boer, P.L. and Smith, D.G., 1994. Orbital forcing and cyclic sequences. *Orbital forcing and cyclic sequences*, pp.1-14

Deschamps, P., Durand, N., Bard, E., Hamelin, B., Camoin, G., Thomas, A.L., Henderson, G.M., Okuno, J.I. and Yokoyama, Y., 2012. Ice-sheet collapse and sea-level rise at the Bølling warming 14,600 years ago. *Nature*, *483*(7391), pp.559-564

Desilets, D. and Zreda, M., 2001. On scaling cosmogenic nuclide production rates for altitude and latitude using cosmic-ray measurements. *Earth and Planetary Science Letters*, *193*(1-2), pp.213-225

Duk-Rodkin, A., 1999. *Glacial limits map of Yukon Territory. Geological Survey of Canada*, Open File, 3694(1). Indian and Northern Affairs Canada Geoscience Map 1999-2. Scale 1:1,000,000

Duk-Rodkin, A., 2022. *Glacial limits, Mackenzie Mountains and foothills, Northwest Territories, Canada*. Geological Survey of Canada, Open File 8891. Scale 1:1,000,000. https://doi.org/10.4095/10.4095/330011

Duk-Rodkin, A. and Barendregt, R.W., 2011. Stratigraphical record of glacials/interglacials in northwest Canada. In *Developments in Quaternary Sciences* (Vol. 15, pp. 661-698). Elsevier

Duk-Rodkin, A. and Hughes, O.L., 1991. Age relationships of Laurentide and montane glaciations, Mackenzie mountains, Northwest territories. *Géographie physique et Quaternaire*, *45*(1), pp.79-90

Duk-Rodkin, A. and Hughes, O.L., 1992. Pleistocene montane glaciations in the Mackenzie Mountains, northwest Territories. *Géographie physique et Quaternaire*, *46*(1), pp.69-83

Duk-Rodkin, A. and Hughes, O.L., 1995. *Quaternary geology of the northeastern part of the central Mackenzie Valley corridor, District of Mackenzie, Northwest Territories*. Geological Survey of Canada

Duk-Rodkin, A., Barendregt, R.W., Tarnocai, C. and Phillips, F.M., 1996. Late Tertiary to late Quaternary record in the Mackenzie Mountains, Northwest Territories, Canada: stratigraphy, paleosols, paleomagnetism, and chlorine-36. *Canadian Journal of Earth Sciences*, *33*(6), pp.875-895

Duk-Rodkin, A., Barendregt, R.W., Tarnocai, C. and Phillips, F.M., 1996. Late Tertiary to late Quaternary record in the Mackenzie Mountains, Northwest Territories, Canada: stratigraphy, paleosols, paleomagnetism, and chlorine-36. *Canadian Journal of Earth Sciences*, *33*(6), pp.875-895

Dulfer, H.E., Margold, M., Darvill, C.M. and Stroeven, A.P., 2022. Reconstructing the advance and retreat dynamics of the central sector of the last Cordilleran Ice Sheet. *Quaternary Science Reviews*, *284*, p.107465

Dulfer, H.E., Margold, M., Engel, Z., Braucher, R. and Aster Team, 2021. Using 10Be dating to determine when the Cordilleran Ice Sheet stopped flowing over the Canadian Rocky Mountains. *Quaternary Research*, *102*, pp.222-233

Dunai, T.J. and Lifton, N.A., 2014. The nuts and bolts of cosmogenic nuclide production. *Elements*, *10*(5), pp.347-350

Dyke, A.S. and Evans, D.J.A., 2014. Ice-marginal terrestrial landsystems: northern Laurentide and Innuitian ice sheet margins. In *Glacial Landsystems* (pp. 143-165). Routledge

Dyke, A.S. and Prest, V.K., 1987. Late Wisconsinan and Holocene history of the Laurentide ice sheet. *Géographie physique et Quaternaire*, *41*(2), pp.237-263

Dyke, A.S., 2004. An outline of North American deglaciation with emphasis on central and northern Canada. *Developments in Quaternary Sciences*, *2*, pp.373-424

Dyke, A.S., Andrews, J.T., Clark, P.U., England, J.H., Miller, G.H., Shaw, J. and Veillette, J.J., 2002. The Laurentide and Innuitian ice sheets during the last glacial maximum. *Quaternary Science Reviews*, *21*(1-3), pp.9-31

Dyke, A.S., Moore, A. and Robertson, L., 2003. Deglaciation of North America

Ely, J.C., Clark, C.D., Hindmarsh, R.C., Hughes, A.L., Greenwood, S.L., Bradley, S.L., Gasson, E., Gregoire, L., Gandy, N., Stokes, C.R. and Small, D., 2021. Recent progress on combining geomorphological and geochronological data with ice sheet modelling, demonstrated using the last British–Irish Ice Sheet. *Journal of Quaternary Science*, *36*(5), pp.946-960

Evans, D.J.A., Lemmen, D.S. and Rea, B.R., 1999. Glacial landsystems of the southwest Laurentide Ice Sheet: modern Icelandic analogues. *Journal of Quaternary Science*, *14*(7), pp.673-691

Evans, D.J.A., Smith, I.R., Gosse, J.C. and Galloway, J.M., 2021. Glacial landforms and sediments (landsystem) of the Smoking Hills area, Northwest Territories, Canada: implications for regional Pliocene–Pleistocene Laurentide Ice Sheet dynamics. *Quaternary Science Reviews*, *262*, p.106958

Fastovich, D., Russell, J.M., Jackson, S.T., Krause, T.R., Marcott, S.A. and Williams, J.W., 2020. Spatial fingerprint of Younger Dryas cooling and warming in eastern North America. *Geophysical Research Letters*, *47*(22), p.e2020GL090031

Fastovich, D., Russell, J.M., Marcott, S.A. and Williams, J.W., 2022. Spatial fingerprints and mechanisms of precipitation and temperature changes during the Younger Dryas in eastern North America. *Quaternary Science Reviews*, 294, p.107724

Fichefet, T., Poncin, C., Goosse, H., Huybrechts, P., Janssens, I. and Le Treut, H., 2003. Implications of changes in freshwater flux from the Greenland ice sheet for the climate of the 21st century. *Geophysical Research Letters*, 30(17)

Field, C.B., Barros, V.R., Dokken, D.J., Mach, K.J., Mastrandrea, M.D., Bilir, T.E., Chatterjee, M., Ebi, K.L., Estrada, Y.O., Genova, R.C., Girma, B., Kissel, E.S., Levy, A.N., MacCracken, S., Mastrandrea, P.R., and White, L.L., 2014. Climate change 2014: impacts, adaptation, and vulnerability. Part A: global and sectoral aspects. Contribution of Working Group II to the Fifth Assessment Report of the Intergovernmental Panel

Froese, D. G., Young, J. M., Norris, S. L., and Margold, M., 2019. Availability and viability of the ice-free corridor and Pacific coast routes for the peopling of the Americas, *The SAA [Society for American Archaeology] Archaeological Record*, 19, pp.27–33.

Fulton, R.J., 1989. *Quaternary geology of Canada and Greenland*. Geological Society of America

Fulton, R. J. 1995. *Surficial materials of Canada*, Ottawa, Ontario: Geological Survey of Canada. "A" Series Map, 1880A, Scale 1:5,000,000.

Gomez, N., Gregoire, L.J., Mitrovica, J.X. and Payne, A.J., 2015. Laurentide-Cordilleran Ice Sheet saddle collapse as a contribution to meltwater pulse 1A. *Geophysical Research Letters*, *42*(10), pp.3954-3962

Gosse, J.C. and Phillips, F.M., 2001. Terrestrial in situ cosmogenic nuclides: theory and application. *Quaternary Science Reviews*, *20*(14), pp.1475-1560

Government of Canada., 2013. Landsat Image Mosaic of Canada. Natural Resources Canada, Canadian Forest Service, Pacific Forestry Centre. Available at https://ftp.maps.canada.ca/pub/nrcan_rncan/archive/image/landsat_7/canada_mosaic/. Accessed 1 April 2021

Government of Canada., 2023. Canadian Climate Normals 1981–2010, Station for Norman Wells and Fort Simpson, https://climate.weather.gc.ca/climate_normals/results_1981_2010_e.html?stnID=1680&autofwd=1. Accessed 27 December 2023.

Greenwood, S.L. and Clark, C.D., 2009. Reconstructing the last Irish Ice Sheet 1: changing flow geometries and ice flow dynamics deciphered from the glacial landform record. *Quaternary Science Reviews*, *28*(27-28), pp.3085-3100

Greenwood, S.L., Clark, C.D. and Hughes, A.L., 2007. Formalising an inversion methodology for reconstructing ice-sheet retreat patterns from meltwater channels: application to the British Ice Sheet. *Journal of Quaternary Science: Published for the Quaternary Research Association*, *22*(6), pp.637-645

Gregoire, L.J., Otto-Bliesner, B., Valdes, P.J. and Ivanovic, R., 2016. Abrupt Bølling warming and ice saddle collapse contributions to the Meltwater Pulse 1a rapid sea level rise. *Geophysical research letters*, *43*(17), pp.9130-9137

Gregoire, L.J., Payne, A.J. and Valdes, P.J., 2012. Deglacial rapid sea level rises caused by ice-sheet saddle collapses. *Nature*, *487*(7406), pp.219-222

Halsted, C.T., Bierman, P.R., Shakun, J.D., Davis, T., Corbett, L.B., Caffee, M.W., Hodgdon, T.S. and Licciardi, J.M., 2023. Rapid southeastern Laurentide Ice Sheet thinning during the last deglaciation revealed by elevation profiles of in situ cosmogenic 10Be. *Bulletin*, *135*(7-8), pp.2075-2087

Hawkins, A.C., Menounos, B., Goehring, B.M., Osborn, G., Pelto, B.M., Darvill, C.M. and Schaefer, J.M., 2023. Late Holocene glacier and climate fluctuations in the Mackenzie and Selwyn Mountain Ranges, Northwest Canada. *The Cryosphere Discussions*, pp.1-26

Heginbottom, J. A., Dubreuil, M.-A., & Harker, P. A.C., 1995. *Permafrost – Canada, National Atlas of Canada MCR 4177, scale 1:7,500,000*. Department of Energy, Mines and Resources Canada.

Heintzman, P.D., Froese, D., Ives, J.W., Soares, A.E., Zazula, G.D., Letts, B., Andrews, T.D., Driver, J.C., Hall, E., Hare, P.G. and Jass, C.N., 2016. Bison phylogeography constrains dispersal and viability of the Ice Free Corridor in western Canada. *Proceedings of the National Academy of Sciences*, *113*(29), pp.8057-8063

Hemming, S.R., 2004. Heinrich events: Massive late Pleistocene detritus layers of the North Atlantic and their global climate imprint. *Reviews of Geophysics*, *42*(1)

Heyman, J., 2024. Expage global compilation of cosmogenic exposure ages. Available at: https://expage.github.io/data.html. Accessed: 02 February 2024.

Heyman, J., Stroeven, A.P., Harbor, J.M. and Caffee, M.W., 2011. Too young or too old: evaluating cosmogenic exposure dating based on an analysis of compiled boulder exposure ages. *Earth and Planetary Science Letters*, *302*(1-2), pp.71-80

Hodder, T.J., Gauthier, M.S., Ross, M. and Lian, O.B., 2023. Was there a nonglacial episode in the western Hudson Bay Lowland during Marine Isotope Stage 3? *Quaternary Research*, *116*, pp.148-161

Hughes, A.L., Clark, C.D. and Jordan, C.J., 2014. Flow-pattern evolution of the last British Ice Sheet. *Quaternary Science Reviews*, *89*, pp.148-168

Huntley, D.H., Hickin, A.S. and Lian, O.B., 2017. The pattern and style of deglaciation at the Late Wisconsinan Laurentide and Cordilleran ice sheet limits in northeastern British Columbia. *Canadian Journal of Earth Sciences*, *54*(1), pp.52-75

Huntley, D.H., Hickin, A.S. and Lian, O.B., 2017. The pattern and style of deglaciation at the Late Wisconsinan Laurentide and Cordilleran ice sheet limits in northeastern British Columbia. *Canadian Journal of Earth Sciences*, *54*(1), pp.52-75

IPCC, 2013. *Climate Change 2013: The Physical Science Basis. Contribution of working group I to the Fifth Assessment Report of the Intergovernmental Panel on Climate Change*. Stocker, T.F., Qin, D., Plattner, G.K., Tignor, M., Allen, S.K., Boschung, J., Nauels, A., Xia, Y., Bex, V., and Midgley, P.M., (eds). Cambridge University Press, Cambridge. United Kingdom and New York.

IPCC, 2019. Summary for Policymakers. In: *IPCC Special Report on the Ocean and Cryosphere in a Changing Climate* [H.-O. Pörtner, D.C. Roberts, V. Masson-Delmotte, P. Zhai, M. Tignor, E. Poloczanska, K. Mintenbeck, A. Alegría, M. Nicolai, A. Okem, J. Petzold, B. Rama, N.M. Weyer (eds.)]. In press.

IPCC, 2023: Summary for Policymakers. In: Climate Change 2023: Synthesis Report. Contribution of Working Groups I, II and III to the Sixth Assessment Report of the Intergovernmental Panel on Climate Change [Core Writing Team, H. Lee and J. Romero (eds.)]. IPCC, Geneva, Switzerland, pp. 1-34, doi:10.59327/IPCC/AR6-9789291691647.001

Ivanovic, R.F., Gregoire, L.J., Wickert, A.D., Valdes, P.J. and Burke, A., 2017. Collapse of the North American ice saddle 14,500 years ago caused widespread cooling and reduced ocean overturning circulation. *Geophysical Research Letters*, *44*(1), pp.383-392

Ivy-Ochs, S. and Briner, J.P., 2014. Dating disappearing ice with cosmogenic nuclides. *Elements*, *10*(5), pp.351-356

Jackson Jr, L.E., Phillips, F.M., Shimamura, K. and Little, E.C., 1997. Cosmogenic 36Cl dating of the Foothills erratics train, Alberta, Canada. *Geology*, *25*(3), pp.195-198

Jones, R.S., Small, D., Cahill, N., Bentley, M.J. and Whitehouse, P.L., 2019. iceTEA: tools for plotting and analysing cosmogenic-nuclide surface-exposure data from former ice margins. *Quaternary Geochronology*, *51*, pp.72-86

Kennedy, K.E., Froese, D.G., Zazula, G.D. and Lauriol, B., 2010. Last Glacial Maximum age for the northwest Laurentide maximum from the Eagle River spillway and delta complex, northern Yukon. *Quaternary Science Reviews*, *29*(9-10), pp.1288-1300

Kleman, J. and Borgström, I., 1996. Reconstruction of palaeo-ice sheets: the use of geomorphological data. *Earth surface processes and landforms*, *21*(10), pp.893-909

Kleman, J., Hättestrand, C., Borgström, I. and Stroeven, A., 1997. Fennoscandian palaeoglaciology reconstructed using a glacial geological inversion model. *Journal of glaciology*, *43*(144), pp.283-299.

Kleman, J., Jansson, K., De Angelis, H., Stroeven, A.P., Hättestrand, C., Alm, G. and Glasser, N., 2010. North American Ice Sheet build-up during the last glacial cycle, 115–21 kyr. *Quaternary Science Reviews*, *29*(17-18), pp.2036-2051

Kokelj, S.V., Lantz, T.C., Tunnicliffe, J., Segal, R. and Lacelle, D., 2017. Climate-driven thaw of permafrost preserved glacial landscapes, northwestern Canada. *Geology*, *45*(4), pp.371-374

Lambeck, K. and Chappell, J., 2001. Sea level change through the last glacial cycle. *Science*, *292*(5517), pp.679-686

Le Treut, H. and Ghil, M., 1983. Orbital forcing, climatic interactions, and glaciation cycles. *Journal of Geophysical Research: Oceans*, *88*(C9), pp.5167-5190

Lemmen, D.S., Duk-Rodkin, A. and Bednarski, J.M., 1994. Late glacial drainage systems along the northwestern margin of the Laurentide Ice Sheet. *Quaternary Science Reviews*, *13*(9-10), pp.805-828

Licciardi, J.M., Clark, P.U., Jenson, J.W. and Macayeal, D.R., 1998. Deglaciation of a soft-bedded Laurentide Ice Sheet. *Quaternary Science Reviews*, *17*(4-5), pp.427-448

Lifton, N., Sato, T. and Dunai, T.J., 2014. Scaling in situ cosmogenic nuclide production rates using analytical approximations to atmospheric cosmic-ray fluxes. *Earth and Planetary Science Letters*, *386*, pp.149-160

Löfverström, M., Caballero, R., Nilsson, J. and Kleman, J., 2014. Evolution of the large-scale atmospheric circulation in response to changing ice sheets over the last glacial cycle. *Climate of the Past*, *10*(4): 1453-1471

Margold, M., Stokes, C.R. and Clark, C.D., 2018. Reconciling records of ice streaming and ice margin retreat to produce a palaeogeographic reconstruction of the deglaciation of the Laurentide Ice Sheet. *Quaternary Science Reviews*, *189*, pp.1-30

Menounos, B., Goehring, B.M., Osborn, G., Margold, M., Ward, B., Bond, J., Clarke, G.K., Clague, J.J., Lakeman, T., Koch, J. and Caffee, M.W., 2017. Cordilleran Ice Sheet mass loss preceded climate reversals near the Pleistocene Termination. *Science*, *358*(6364), pp.781-784

Miller, G.H. and Andrews, J.T., 2019. Hudson Bay was not deglaciated during MIS-3. *Quaternary Science Reviews*, *225*, p.105944

Morlan, R.E., Nelson, D.E., Brown, T.A., Vogel, J.S. and Southon, J.R., 1990. Accelerator mass spectrometry dates on bones from Old Crow Basin, northern Yukon Territory. *Canadian Journal of Archaeology/Journal Canadien d'Archéologie*, pp.75-92

Murton, J.B., Waller, R.I., Hart, J.K., Whiteman, C.A., Pollard, W.H. and Clark, I.D., 2004. Stratigraphy and glaciotectonic structures of permafrost deformed beneath the northwest margin of the Laurentide ice sheet, Tuktoyaktuk Coastlands, Canada. *Journal of Glaciology*, *50*(170), pp.399-412

Murton, J.B., Whiteman, C.A., Waller, R.I., Pollard, W.H., Clark, I.D. and Dallimore, S.R., 2005. Basal ice facies and supraglacial melt-out till of the Laurentide Ice Sheet, Tuktoyaktuk Coastlands, western Arctic Canada. *Quaternary Science Reviews*, *24*(5-6), pp.681-708

Murton, JB, Bateman, MD, Waller, RI and Whiteman, CA, 2015, September. Late Wisconsin glaciation of Hadwen and Summer islands, Tuktoyaktuk Coastlands, NWT, Canada. In *GEOQuébec2015: 7th Canadian Permafrost Conference* (pp. 20-23)

Norris, S.L., Margold, M. and Froese, D.G., 2017. Glacial landforms of northwest Saskatchewan. *Journal of Maps*, *13*(2), pp.600-607

Norris, S.L., Margold, M., Evans, D.J., Atkinson, N. and Froese, D.G., 2023. Dynamical response of the southwestern Laurentide Ice Sheet to rapid Bølling-Allerød warming. *The Cryosphere Discussions*, pp.1-32

Norris, S.L., Tarasov, L., Monteath, A.J., Gosse, J.C., Hidy, A.J., Margold, M. and Froese, D.G., 2022. Rapid retreat of the southwestern Laurentide Ice Sheet during the Bølling-Allerød interval. *Geology*, *50*(4), pp.417-421

Peel, M.C., Finlayson, B.L. and McMahon, T.A., 2007. Updated world map of the Köppen-Geiger climate classification. *Hydrology and earth system sciences*, *11*(5), pp.1633-1644

Persaud, B.D., 2023. Spatial and temporal characteristics of historical surface climate over the Northwest Territories, Canada. (PhD thesis, Wilfrid Laurier University).

Phillips, D. W., 1990. The climates of Canada. Ottawa, Ont: Supply and Services Canada.

Phillips, F.M., Bowen, D.Q. and Elmore, D., 1994. Surface exposure dating of glacial features in Great Britain using cosmogenic chlorine-36: preliminary results. *Mineralogical Magazine A*, *58*, pp.722-723

Pico, T., Creveling, J.R. and Mitrovica, J.X., 2017. Sea-level records from the US mid-Atlantic constrain Laurentide Ice Sheet extent during Marine Isotope Stage 3. *Nature Communications*, *8*(1), p.15612

Plug, L.J., Gosse, J.C., McIntosh, J.J. and Bigley, R., 2007. Attenuation of cosmic ray flux in temperate forest. *Journal of Geophysical Research: Earth Surface*, *112*(F2)

Porter, C., Morin, P., Howat, I., Noh, M. J., Bates, B., Peterman, K., Keesey, S., Schlenk, M., Gardiner, J., Tomko, K., Willis, M., Kelleher, C., Cloutier, M., Husby, E., Foga, S., Nakamura, H., Platson, M., Wethington, M., Williamson, C., Bojesen, M. (2018). ArcticDEM. Available at https://doi.org/10.7910/DVN/OHHUKH. Harvard Dataverse, V1. Accessed on 1 April 2021

Punkari, M., 1980. The ice lobes of the Scandinavian ice sheet during the deglaciation in Finland. *Boreas*, *9*(4), pp.307-310

Rampton, V. N., 1988. Quaternary geology of the Tuktoyaktuk coastlands, Northwest Territories. Geological survey of Canada. *Memoir*, *423*), https://doi.org/10.4095/126937

Randle, M. and Eckersley, R., 2015. Public perceptions of future threats to humanity and different societal responses: A cross-national study. *Futures*, *72*, pp.4-16

Rasmussen, S.O., Bigler, M., Blockley, S.P., Blunier, T., Buchardt, S.L., Clausen, H.B., Cvijanovic, I., Dahl-Jensen, D., Johnsen, S.J., Fischer, H. and Gkinis, V., 2014. A stratigraphic framework for abrupt climatic changes during the Last Glacial period based on three synchronized Greenland ice-core records: refining and extending the INTIMATE event stratigraphy. *Quaternary Science Reviews*, 106:14-28

Reyes, A.V., Carlson, A.E., Milne, G.A., Tarasov, L., Reimink, J.R. and Caffee, M.W., 2022. Revised chronology of northwest Laurentide ice-sheet deglaciation from 10Be exposure ages on boulder erratics. *Quaternary Science Reviews*, 277, p.107369

Rignot, E., Mouginot, J., Morlighem, M., Seroussi, H. and Scheuchl, B., 2014. Widespread, rapid grounding line retreat of Pine Island, Thwaites, Smith, and Kohler glaciers, West Antarctica, from 1992 to 2011. *Geophysical Research Letters*, 41(10), pp.3502-3509

Robel, A.A. and Tziperman, E., 2016. The role of ice stream dynamics in deglaciation. *Journal of Geophysical Research: Earth Surface*, *121*(8), pp.1540-1554

Schaefer, J.M., Codilean, A.T., Willenbring, J.K., Lu, Z.T., Keisling, B., Fülöp, R.H. and Val, P., 2022. Cosmogenic nuclide techniques. *Nature Reviews Methods Primers*, *2*(1), p.18

Schildgen, T.F., Phillips, W.M. and Purves, R.S., 2005. Simulation of snow shielding corrections for cosmogenic nuclide surface exposure studies. *Geomorphology*, *64*(1-2), pp.67-85

Sharpe, D.R., Lesemann, J.E., Knight, R.D. and Kjarsgaard, B.A., 2021. Regional stagnation of the western Keewatin ice sheet and the significance of meltwater corridors and eskers, northern Canada. *Canadian Journal of Earth Sciences*, *58*(10), pp.1005-1026

Small, D., Bentley, M.J., Jones, R.S., Pittard, M.L. and Whitehouse, P.L., 2019. Antarctic ice sheet palaeo-thinning rates from vertical transects of cosmogenic exposure ages. *Quaternary Science Reviews*, *206*, pp.65-80

Smith, I.R., 2002. *Surficial Geology, Mount Merrill (95C/02), Yukon Territory – British Columbia*; Geological Survey of Canada, Open File 4324, 1 map, scale 1:50,000

Smith, I.R., Deblonde, C., Hagedorn, G. and Paulen, R.C., 2023. A drift isopach model for the southwestern Great Slave Lake region, Northwest Territories, Canada. *Journal of Maps*, *19*(1), p.2147871

Smith, M.J. and Pain, C.F., 2011. Geomorphological mapping. *The SAGE Handbook of Geomorphology. SAGE Publications, London*, pp.142-153

Smith, M.J., Rose, J. and Booth, S., 2006. Geomorphological mapping of glacial landforms from remotely sensed data: an evaluation of the principal data sources and an assessment of their quality. *Geomorphology*, *76*(1-2), pp.148-165

Staiger, J., Gosse, J., Toracinta, R., Oglesby, B., Fastook, J. and Johnson, J.V., 2007. Atmospheric scaling of cosmogenic nuclide production: climate effect. *Journal of Geophysical Research: Solid Earth*, *112*(B2)

Stoker, B.J., Margold, M., Gosse, J.C., Hidy, A.J., Monteath, A.J., Young, J.M., Gandy, N., Gregoire, L.J., Norris, S.L. and Froese, D., 2022. The collapse of the Cordilleran–Laurentide ice saddle and early opening of the Mackenzie Valley, Northwest Territories, Canada, constrained by 10 Be exposure dating. *The Cryosphere*, *16*(12), pp.4865-4886

Stokes, C.R. and Clark, C.D., 2003. The Dubawnt Lake palaeo-ice stream: evidence for dynamic ice sheet behaviour on the Canadian Shield and insights regarding the controls on ice-stream location and vigour. *Boreas*, *32*(1), pp.263-279

von Blanckenburg, F. and Willenbring, J.K., 2014. Cosmogenic nuclides: Dates and rates of Earth-surface change. *Elements*, *10*(5), pp.341-346

Wickert, A.D., Mitrovica, J.X., Williams, C. and Anderson, R.S., 2013. Gradual demise of a thin southern Laurentide ice sheet recorded by Mississippi drainage. *Nature*, *502*(7473), pp.668-671

Young, N.E., Briner, J.P., Schaefer, J.M., Miller, G.H., Lesnek, A.J., Crump, S.E., Thomas, E.K., Pendleton, S.L., Cuzzone, J., Lamp, J. and Zimmerman, S., 2020. Reply to Carlson (2020) comment on "Deglaciation of the Greenland and Laurentide ice sheets interrupted by glacier advance during abrupt coolings". *Quaternary Science Reviews*, *240*, p.106354

Young, N.E., Lesnek, A.J., Cuzzone, J.K., Briner, J.P., Badgeley, J.A., Balter-Kennedy, A., Graham, B.L., Cluett, A., Lamp, J.L., Schwartz, R. and Tuna, T., 2021. In situ cosmogenic 10 Be–14 C–26 Al measurements from recently deglaciated bedrock as a new tool to decipher changes in Greenland Ice Sheet size. *Climate of the Past*, *17*(1), pp.419-450

Young, N.E., Schaefer, J.M., Briner, J.P. and Goehring, B.M., 2013. A $^{10}$Be production-rate calibration for the Arctic. *Journal of Quaternary Science*, *28*(5), pp.515-526

Yu, Z. and Wright Jr, H.E., 2001. Response of interior North America to abrupt climate oscillations in the North Atlantic region during the last deglaciation. *Earth-Science Reviews*, *52*(4), pp.333-369

Zazula, G.D., Duk-Rodkin, A., Schweger, C.E. and Morlan, R.E., 2004. Late Pleistocene chronology of glacial Lake Old Crow and the north-west margin of the Laurentide Ice Sheet. In *Developments in quaternary sciences* (Vol. 2, pp. 347-362). Elsevier